Electromagnetic Properties of Antihydrogen and the the Antiproton: Recent results from ALPHA and BASE

Daniel Maxwell
ALPHA Collaboration

Antiprotons at CERN

The antiproton decelerator (AD) provides ~2x10^7 antiprotons every 120 s at ~5 MeV.

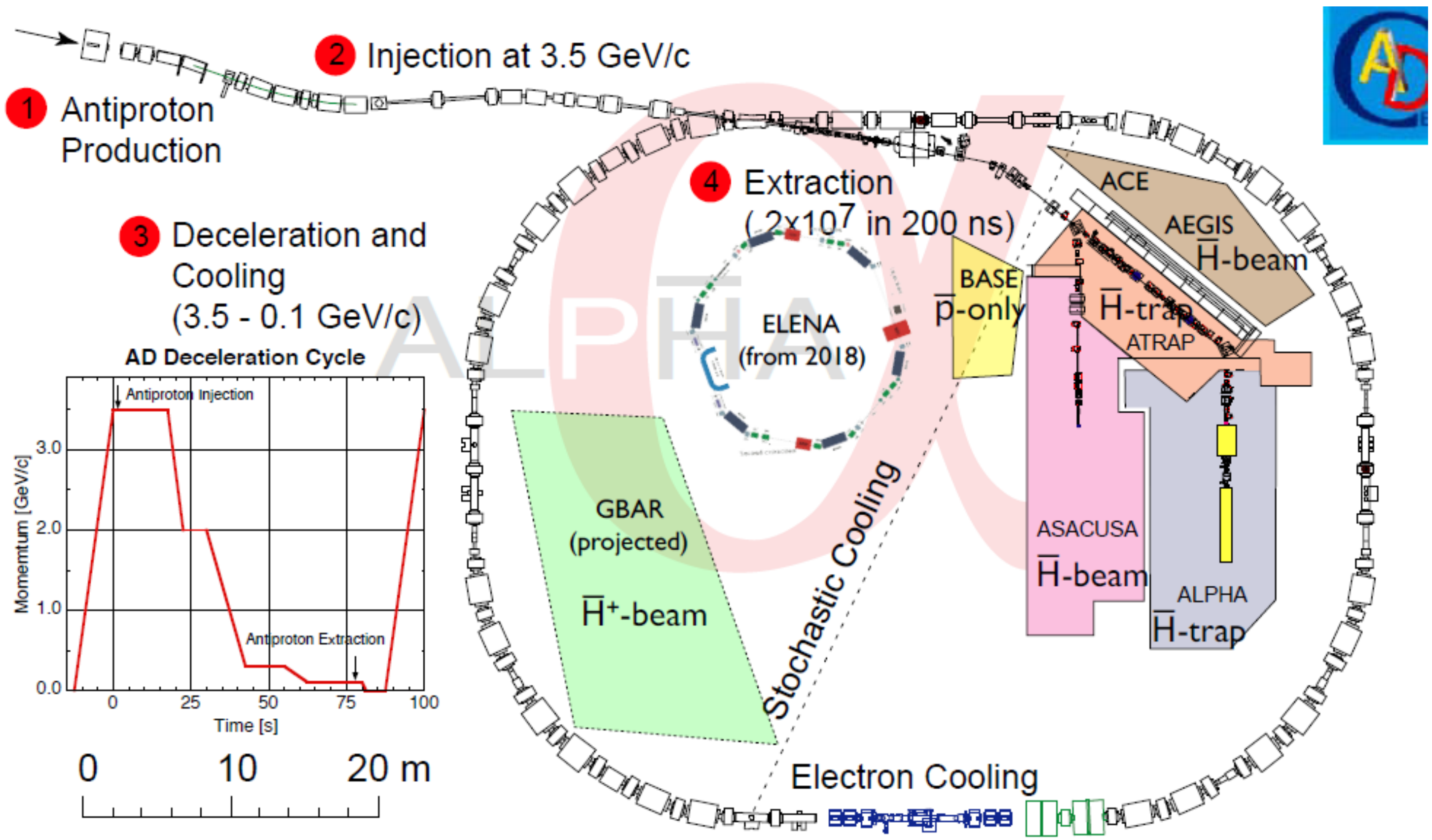

S. Maury *et al.*, Hyp. Int. **109**, 43 (1997).

Summary of AD physics

- Aim: Tests of CPT invariance and the weak equivalence principle through direct measurements on antimatter.
- Motivation: Search for evidence of physics beyond the standard model, insight into the matter/antimatter asymmetry problem.

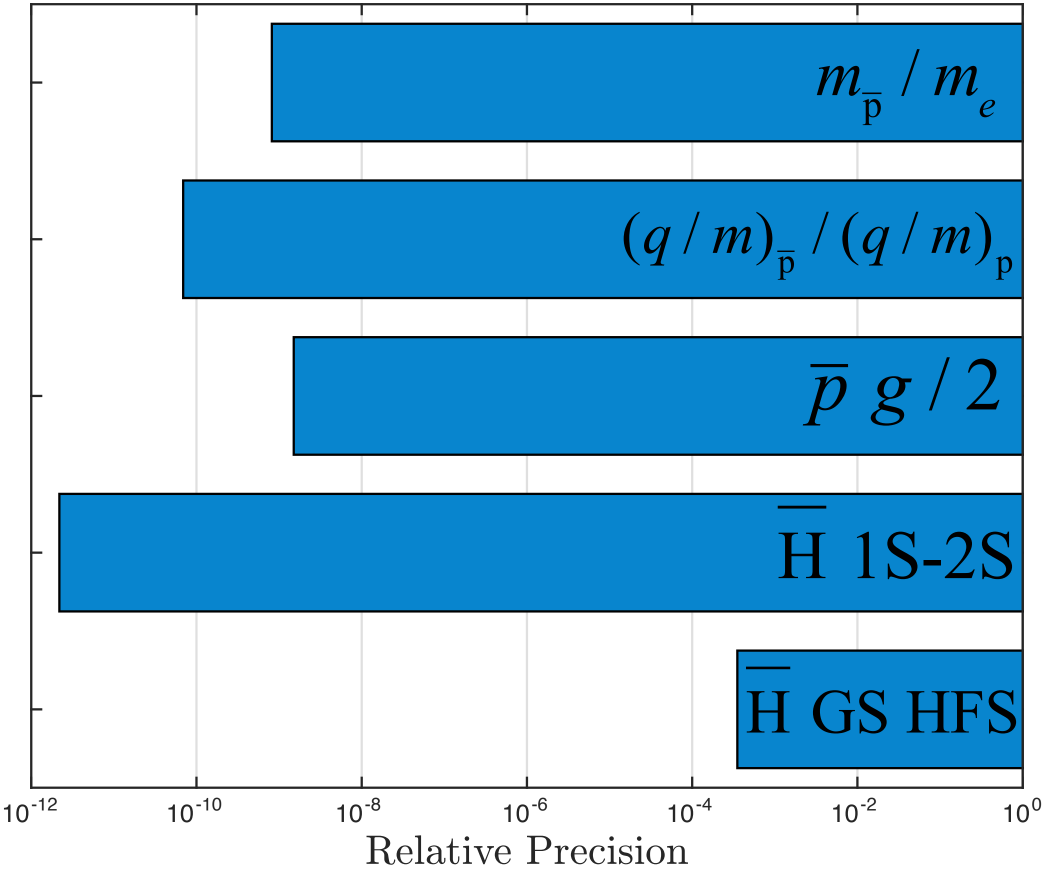

ASACUSA — M. Hori *et al.*, Science **354**, 610 (2016)

BASE — S. Ulmer *et al.*, Nature **524**, 196 (2015)

BASE — C. Smorra *et al.*, Nature **550**, 371 (2017); J. DiSciacca, Phys. Rev. Lett. 110, 130801 (2013) **(ATRAP)**

ALPHA — M. Ahmadi *et al.*, Nature **557**, 71 (2018).

ALPHA — M. Ahmadi *et al.*, Nature **548**, 66 (2017).

Talk Outline

- Recent results from BASE: measurement of antiproton magnetic moment.

- Recent results from ALPHA: measurement of antihydrogen 1S-2S lineshape, and antihydrogen ground-state hyperfine splitting.

- Outlook for antihydrogen physics at ALPHA.

BASE overview

Observation of spin flips with a single trapped proton

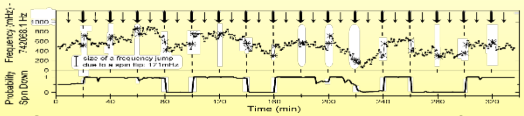

S. Ulmer, et al., **PRL 106, 253001 (2011)**
A. Mooser, et al., **PRL 110, (2013)**

Proton g-factor measurment

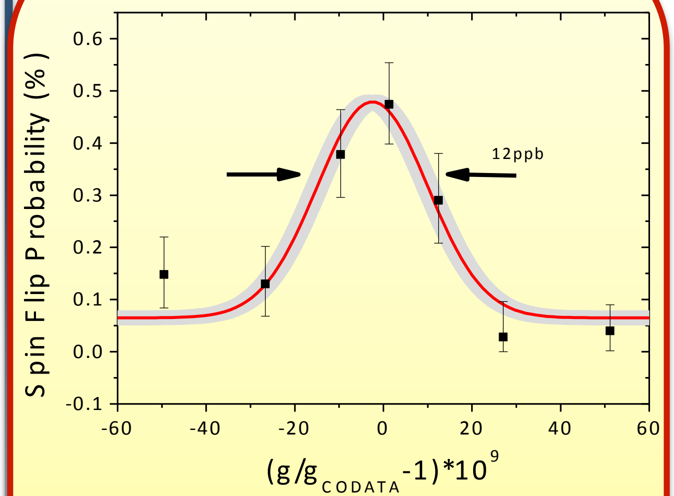

A. Mooser, S. Ulmer, K. Blaum, K. Franke, H. Kracke, C. Leiteritz, W. Quint, C. Smorra, J.Walz, **Nature 509, 596 (2014)**

$g/2 = 2.792847350\ (7)\ (6)$

First direct high precision measurement of the proton magnetic moment.

Precise CPT test with baryons

S. Ulmer, et al., **Nature 524, 196 (2015)**

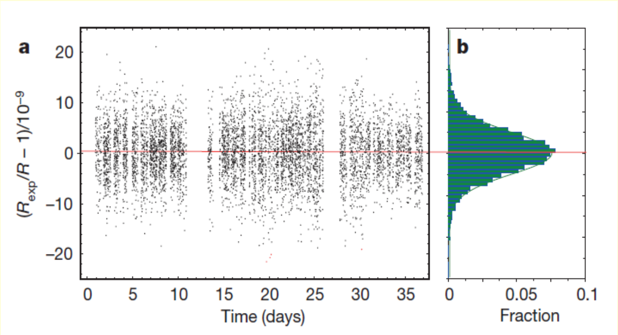

$$1 + \frac{(q/m)_{\bar{p}}}{(q/m)_{p}} = 1(69) \times 10^{-12}$$

$R_{exp,c}$ = 1.001 089 218 755 (64) (26)

To be improved by another factor of 10 to 100

Reservoir trap for antiprotons

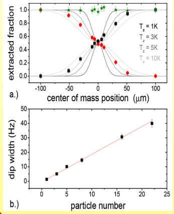

C. Smorra, et al., **Int. Journ. Mass Spec. 389, 10 (2015).**

Idea: Enable operation with antiprotons independent of accelerator run times.

Most precise antiproton g-factor measurement

H. Nagahama, et al., **Nature Comms. 8, 14084 (2017)**
C. Smorra *et al.*, Nature **550**, 371 (2017)

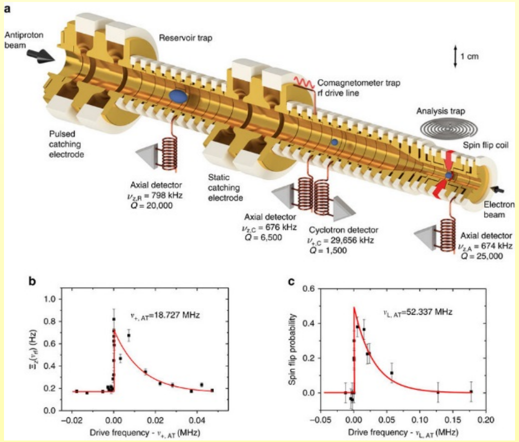

$g/2 = 2.7928465\ (23)$

Sixfold improvement compared to previous measurement

$g/2 = 2.792\ 847\ 344\ 1\ (42)$

350-fold improvement compared to previous measurement

Penning Trap

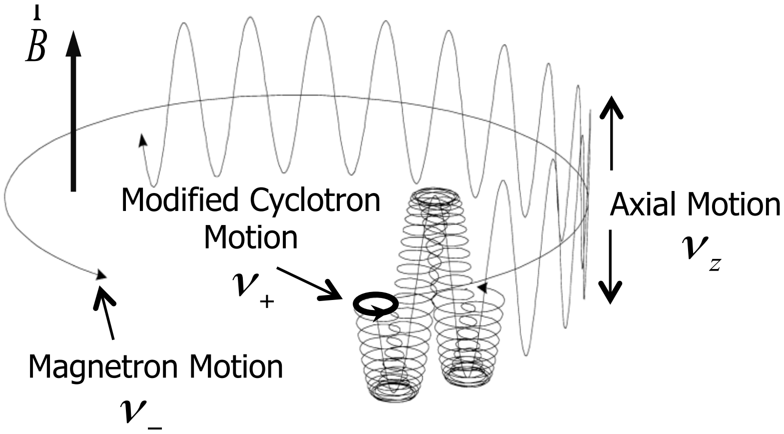

Axial	$\nu_z = 680\,\mathrm{kHz}$
Magnetron	$\nu_- = 8\,\mathrm{kHz}$
Modified Cyclotron	$\nu_+ = 28,9\,\mathrm{MHz}$

Invariance relation: $\nu_c = \sqrt{\nu_+^2 + \nu_-^2 + \nu_z^2}$

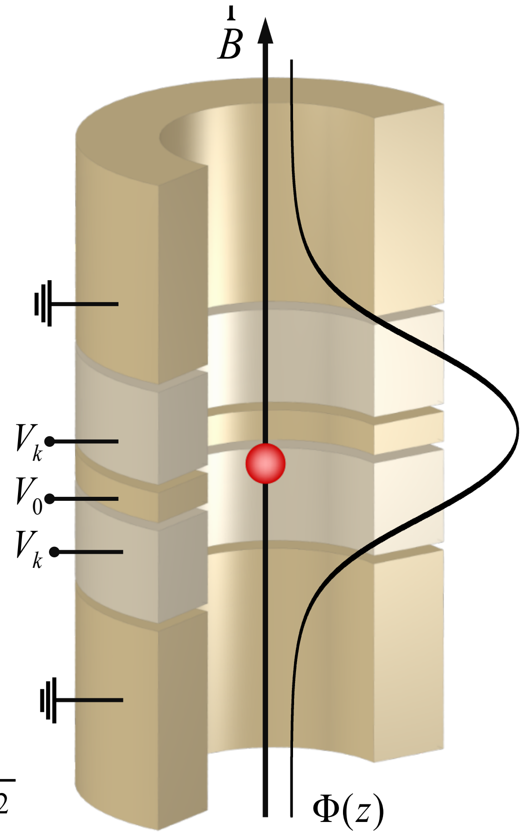

Penning Trap

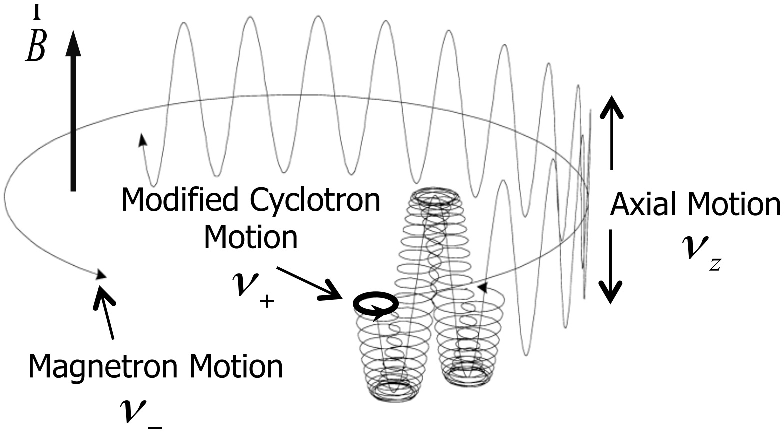

Axial	$\nu_z = 680\,\mathrm{kHz}$
Magnetron	$\nu_- = 8\,\mathrm{kHz}$
Modified Cyclotron	$\nu_+ = 28{,}9\,\mathrm{MHz}$

Invariance relation: $\nu_c = \sqrt{\nu_+^2 + \nu_-^2 + \nu_z^2}$

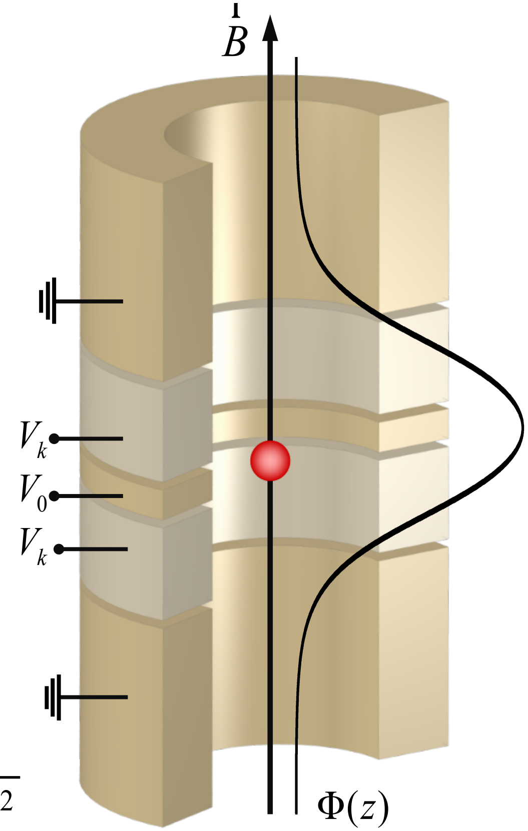

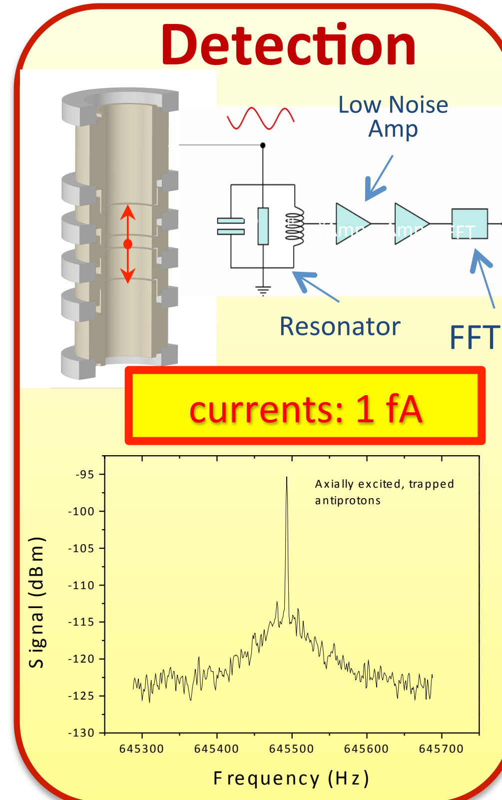

Cyclotron Motion

(Image-current measurements)

$$\omega_c = \frac{q}{m_p} B$$

Larmor Precession

(Continuous Stern Gerlach effect)

$$\omega_L = g \frac{q}{2m_p} B$$

The ratio of these frequencies gives g, the magnetic moment in units of μ_N.

$$\frac{\omega_L}{\omega_c} = \frac{g_{\bar{p}}}{2} = \frac{\mu_{\bar{p}}}{\mu_N}$$

Magnetic Moment Measurements

Use the continuous Stern Gerlach effect:

- A highly inhomogeneous magnetic field is super-imposed on the Penning Trap (a “magnetic bottle”). $B_z = B_0 + B_2(z^2 - \frac{\rho^2}{2})$

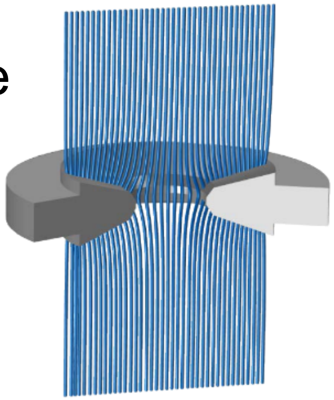

- Energy of magnetic dipole in magnetic field: $\Phi_M = -(\vec{\mu}_p \cdot \vec{B})$

- Inhomogeneity leads to spin-dependent quadratic axial potential – axial frequency depends on spin state. $\Delta\nu_z \sim \frac{\mu_{\bar{p}} B_2}{m_{\bar{p}} \nu_z}$

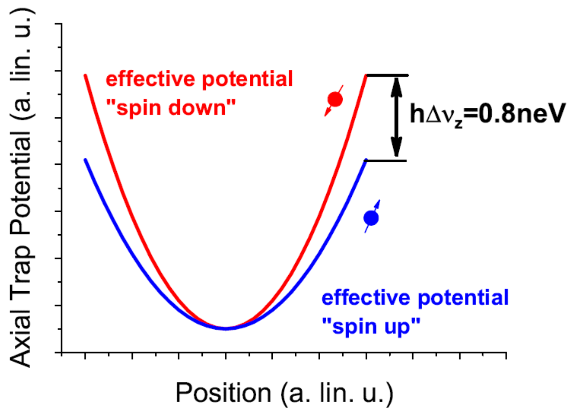

Magnetic Moment Measurements

Use the continuous Stern Gerlach effect:

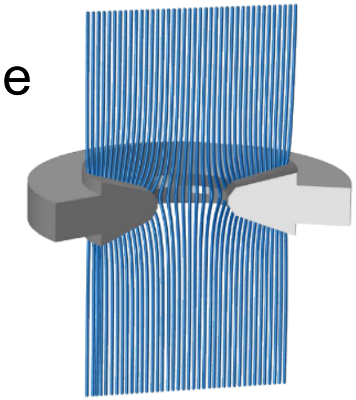

- A highly inhomogeneous magnetic field is super-imposed on the Penning Trap (a “magnetic bottle”). $B_z = B_0 + B_2(z^2 - \frac{\rho^2}{2})$

- Energy of magnetic dipole in magnetic field: $\Phi_M = -(\vec{\mu}_p \cdot \vec{B})$

- Inhomogeneity leads to spin-dependent quadratic axial potential – axial frequency depends on spin state.

$$\Delta\nu_z \sim \frac{\mu_{\bar{p}} B_2}{m_{\bar{p}} \nu_z}$$

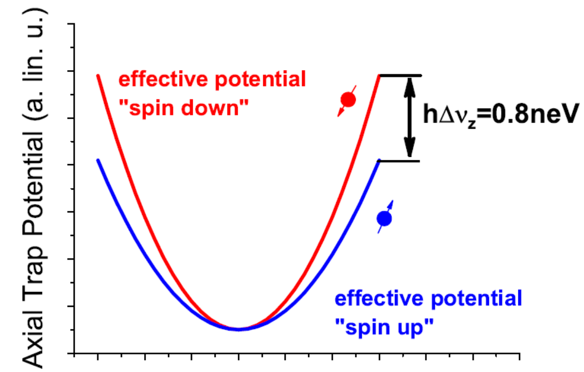

- Very challenging for proton/antiproton system:

$$B_2 \sim 3\times 10^5\ \mathrm{T/m^2} \rightarrow \Delta\nu_z \sim 170\ \mathrm{mHz}$$

- Spin-flips are driven using a RF-field, and the resulting axial frequency shift measured.

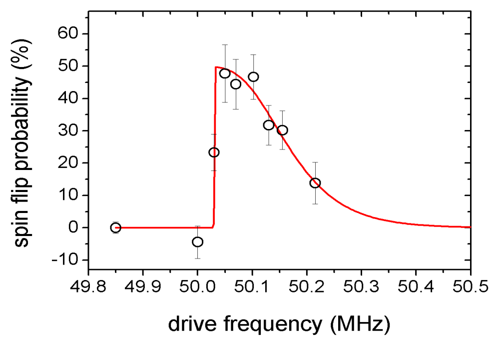

S. Ulmer, A. Mooser *et al.* PRL 106, 253001 (2011)

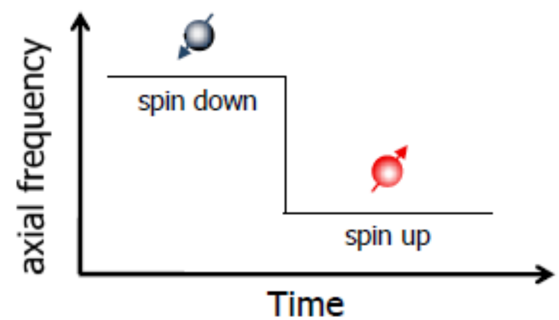

0.8 p.p.m Measurement

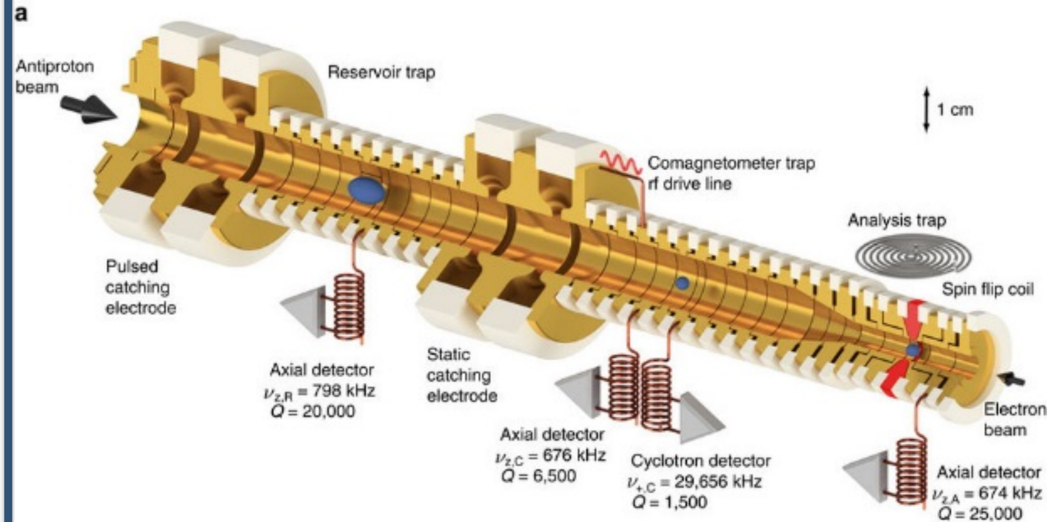

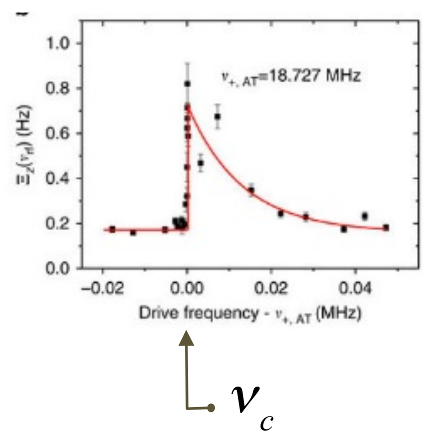

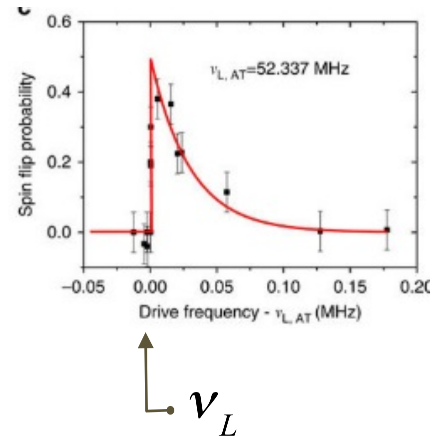

Resolve these frequencies to determine $g_{\bar{p}}$

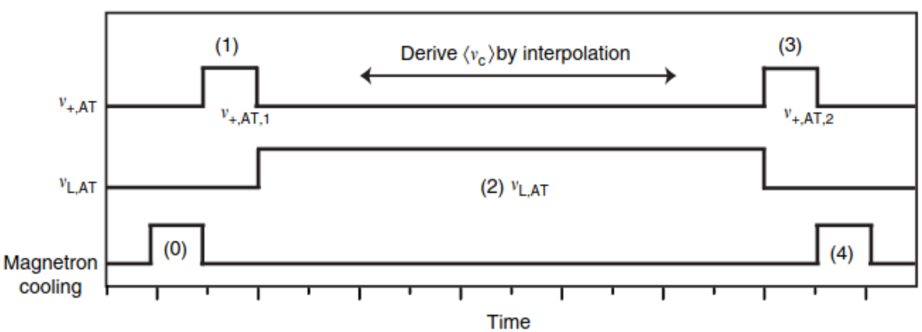

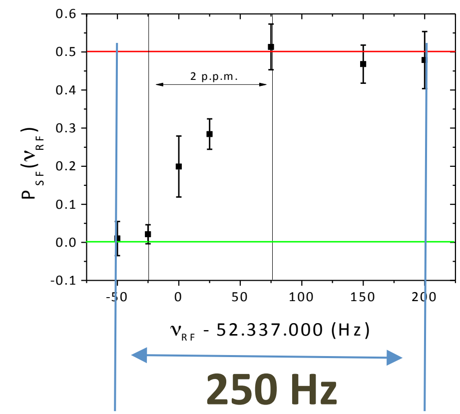

0.8 p.p.m Measurement

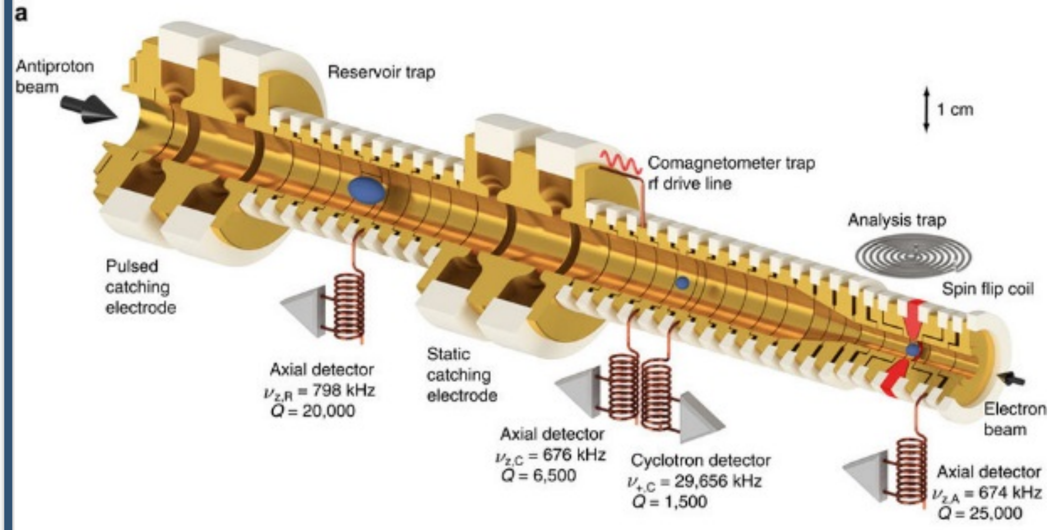

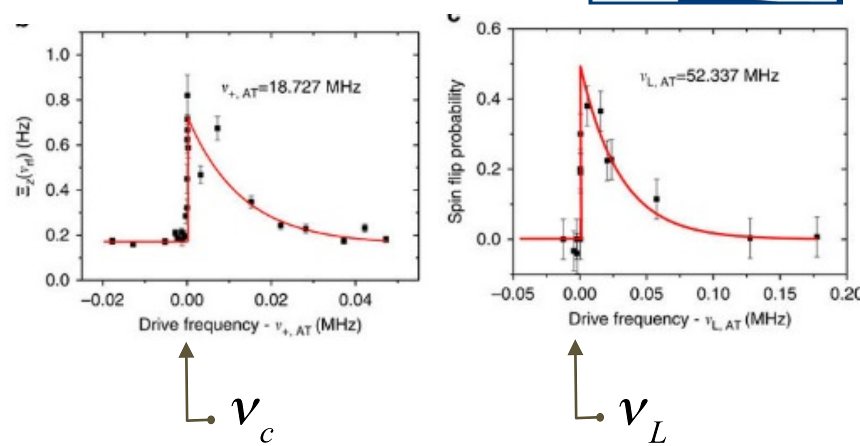

Resolve these frequencies to determine $g_{\bar{p}}$

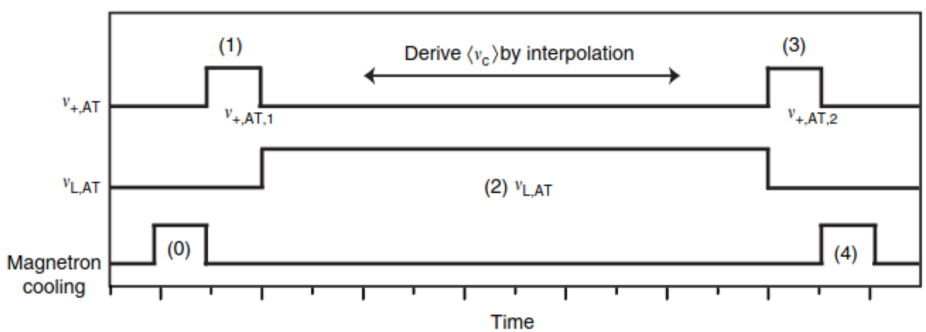

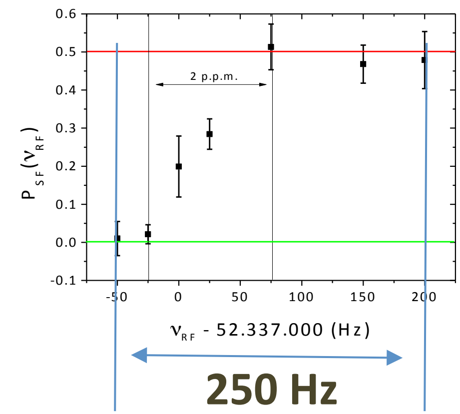

- 6-fold improvement on previous best measurement.

J DiSciacca *et al.* (ATRAP), Phys. Rev. Lett. **110**, 130801 (2013).

- The sharpness of slope of the onset of the resonances is limited by a random walk in the magnetron mode, changing the magnetic field sampled.

$$\frac{g_{\bar{p}}}{2} = 2.7928465\ (23)$$

H. Nagahama *et al.*, Nat. Commun. **8**, 14084 (2017)

Double-Penning Trap, Two-Particle Method

Measure spin flip probability as a function of drive frequency in the homogeneous magnetic field of the precision trap.

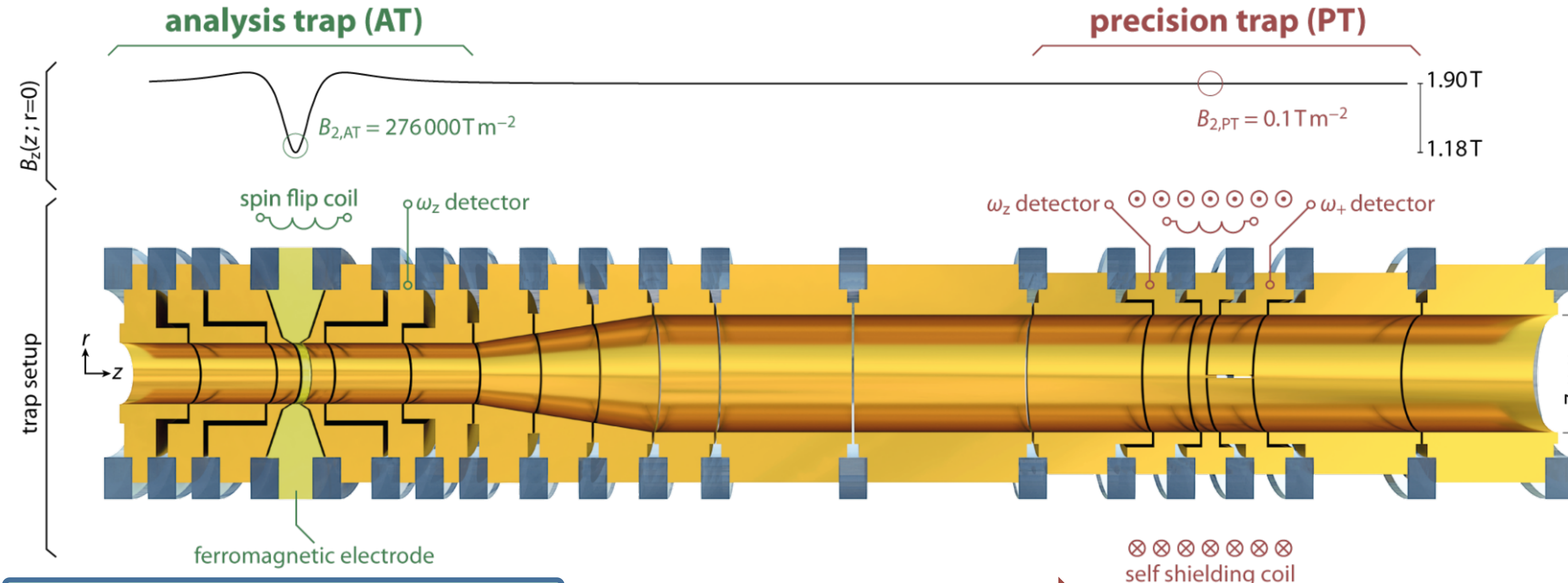

Initialize the spin state

analyze the spin state

particle transport

1) Measure cyclotron ν_c

2) Drive spin transition at ν_{rf}

no spin-flip in PT

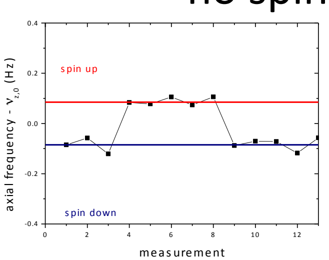

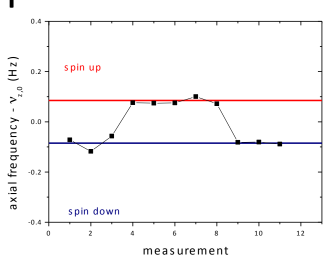

spin-flip in PT

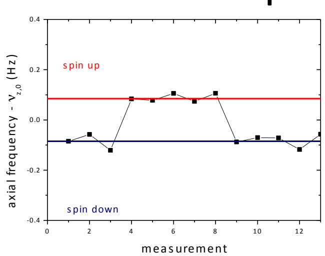

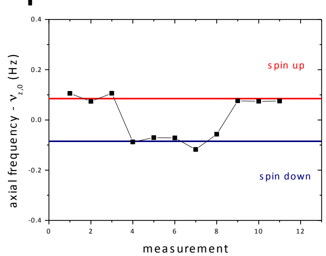

Spin-state resolution

To conclude in which quantum state the particle returns / leaves from precision trap, the double trap method requires high-fidelity **single spin-flip** resolution.

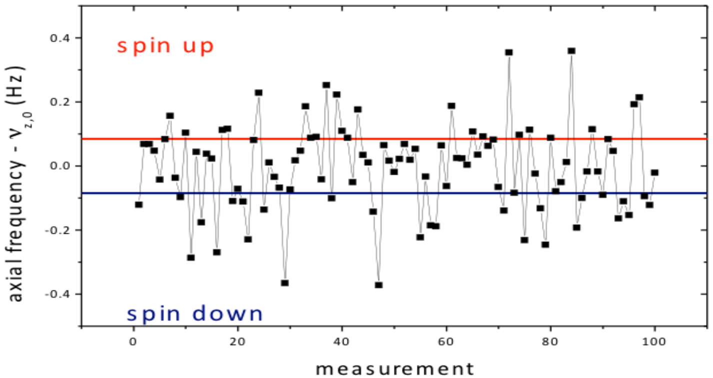

Hot cyclotron particle (1 K)

SSF not resolved

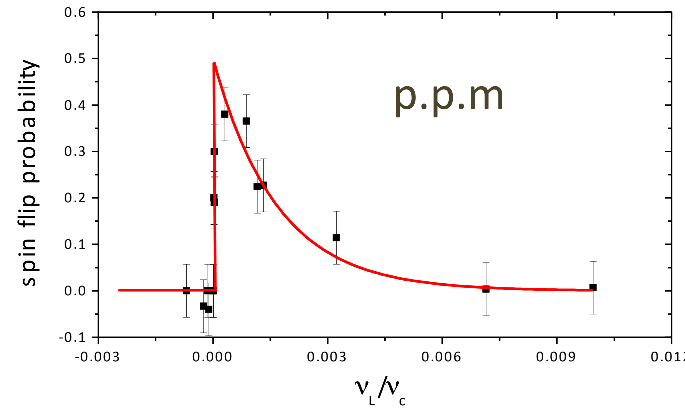

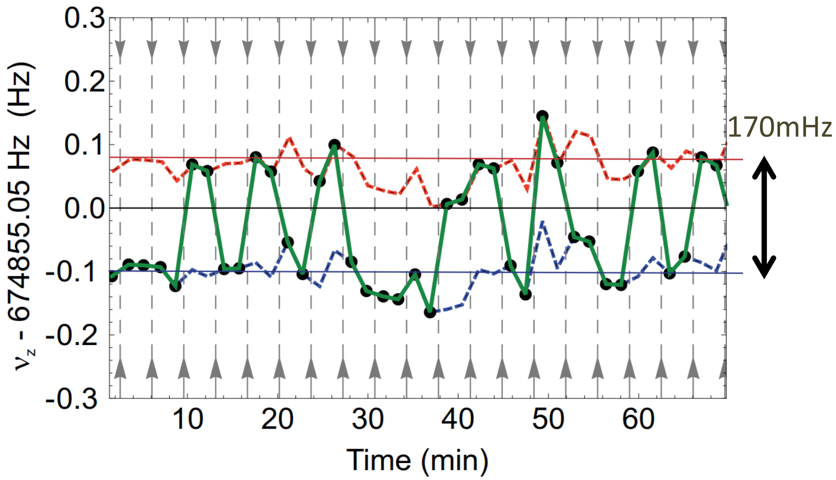

Cold cyclotron particle (50 mK)

SSF resolved

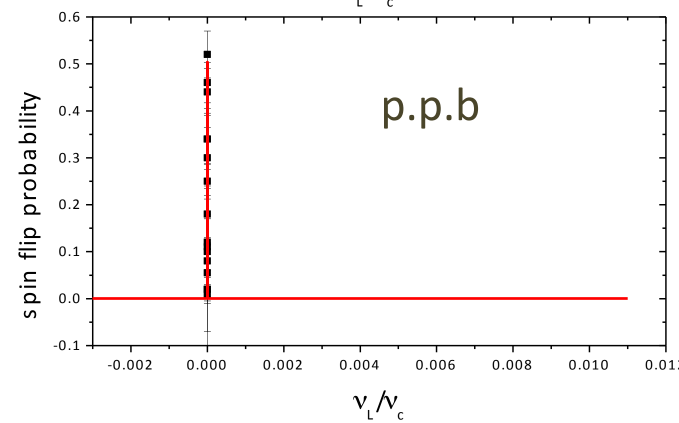

The cyclotron energy of the Lamor particle must be < 0.2 K, otherwise axial frequency fluctuations in the analysis trap are too large to resolve SSF.

The magnetic moment of the antiproton

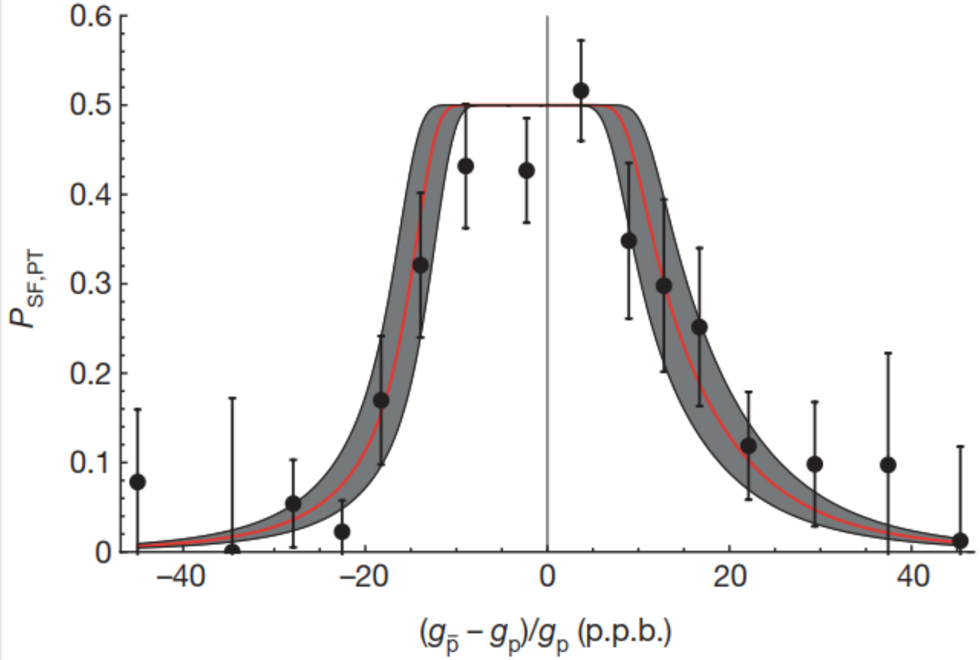

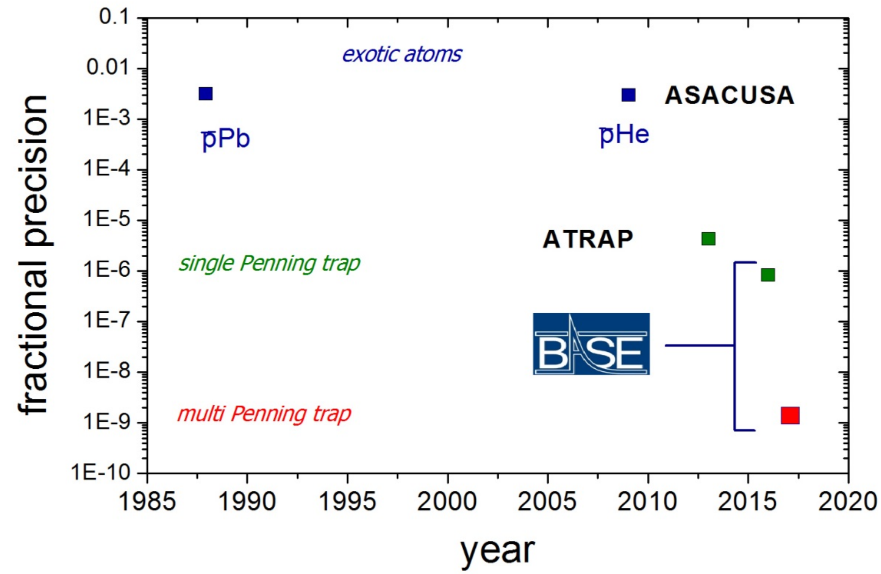

$$\frac{g_{\bar{p}}}{2} = 2.7928473441\ (42)$$

C. Smorra *et al.*, Nature **550**, 371 (2017)

$$\frac{g_p}{2} = 2.79284734462\ (82)$$

G. Schneider *et al.*, Science **358**, 1081 (2017)

- 1.5 p.p.b measurement of the antiproton g-factor.
- In agreement with the proton g–factor, measured to 0.3 p.p.b.

BASE collaboration

Slides provided by BASE spokesperson, Stefan Ulmer.

S. Ulmer
RIKEN

C. Smorra
CERN / RIKEN

S. Sellner
RIKEN

H. Nagahma
RIKEN / Tokyo

T. Higuchi
RIKEN /
Tokyo

J. Harrington
RIKEN & MPIK

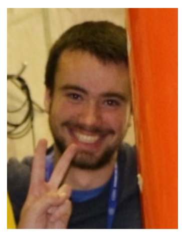

M. Borchert
U - Hannover

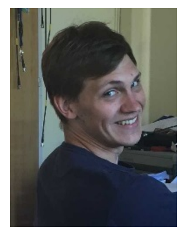

J. Morgner
Hannover / RIKEN

A. Mooser
RIKEN

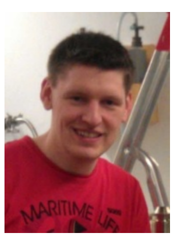

G. Schneider
U - Mainz

M. Bohman
RIKEN/MPIK

M. Wiesinger
RIKEN/MPIK

K. Blaum, Y. Matsuda,
C. Ospelkaus, W. Quint,
J. Walz, Y. Yamazaki

ALPHA Overview

The goal of the ALPHA experiment is to perform precision comparisons of the properties of antihydrogen with those of hydrogen.

Milestones:

- 2010: Trapped antihydrogen. — G. B Andresen *et al.*, Nature **468**, 673 (2010).
- 2010: Antihydrogen confinement for 1000s. — G. B Andresen *et al.*, Nat. Phys. **7**, 558 (2011).
- 2011: Observation of microwave driven spin-flips. — C. Amole *et al.*, Nature **483**, 439 (2012).
- 2016: Observation of the 1S-2S transition. — M. Ahmadi *et al.*, Nature **541**, 506 (2017).
- 2016: Measurement of the ground-state hyperfine splitting. — M. Ahmadi *et al.*, Nature **548**, 66 (2017).
- 2017: Characterisation of the 1S-2S transition lineshape. — M. Ahmadi *et al.*, Nature **557**, 71 (2018).

ALPHA-1 apparatus
ALPHA-2 apparatus

ALPHA-2 Apparatus

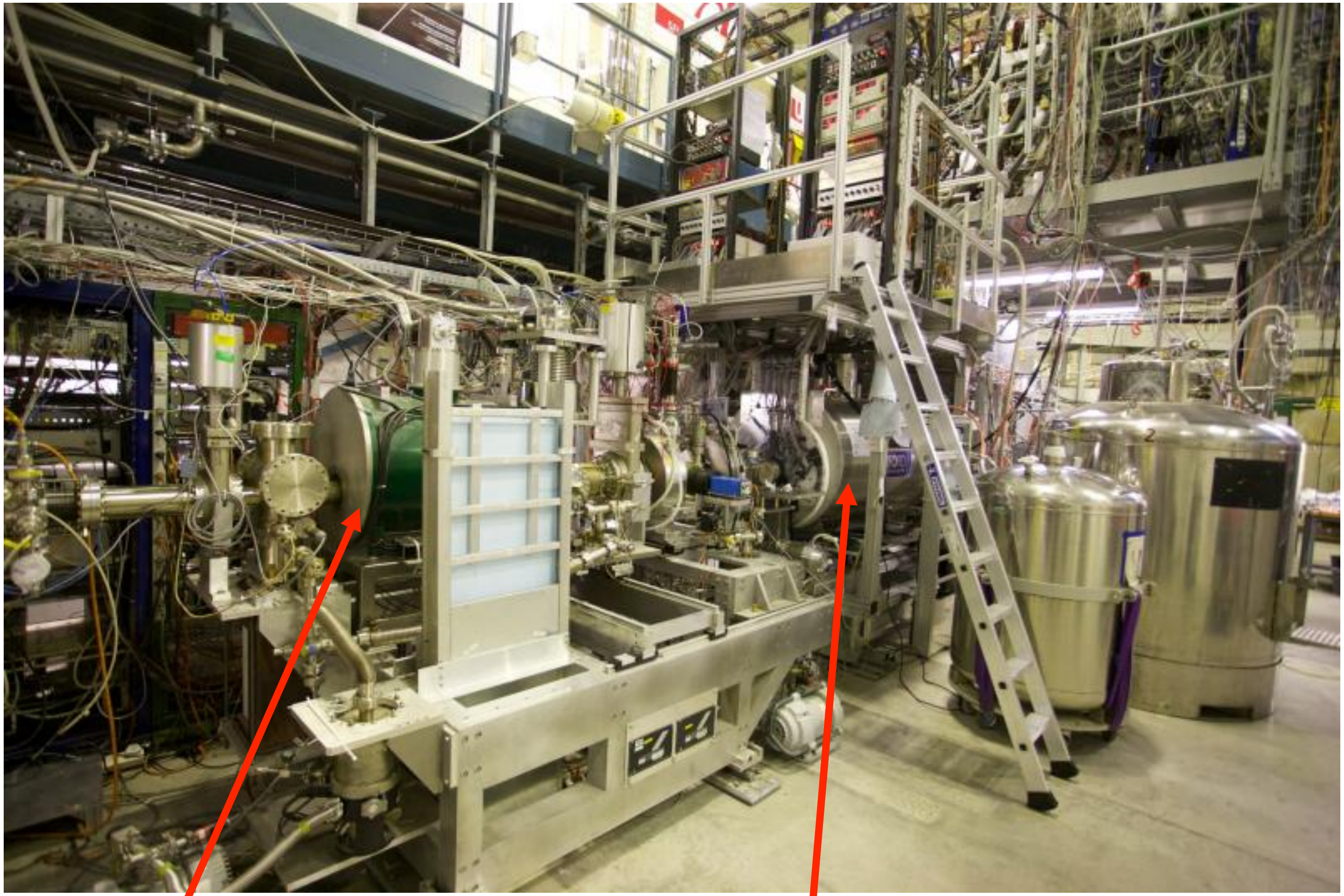

Antiproton "catching trap" Antihydrogen "atom trap"

Antihydrogen synthesis

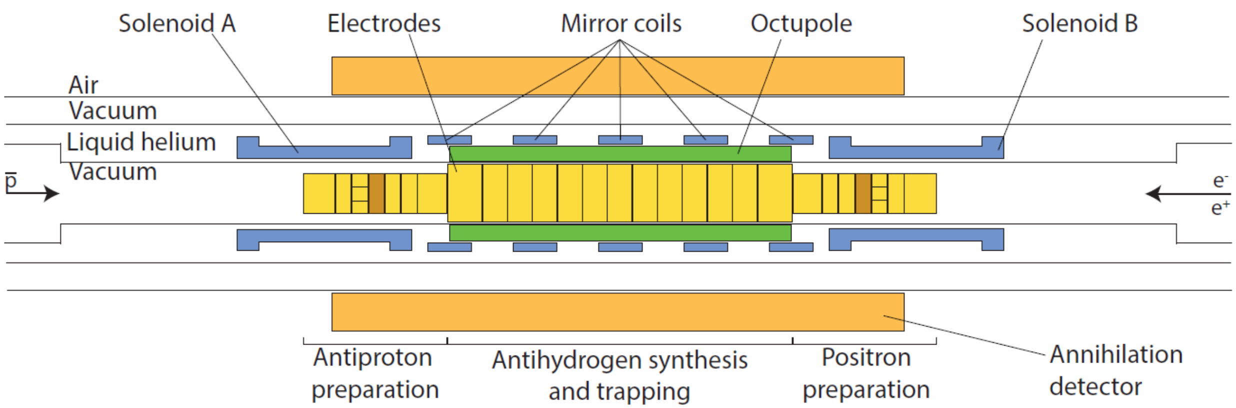

Trap positrons and antiprotons in adjacent potential wells of a Penning-Malmberg trap.

- Slowly merge the particles (in 1s) by lowering the barrier between them.
- We typically mix 3 million positrons (at ~20K) with 90,000 antiprotons (at ~50K) forming around 50,000 antihydrogen atoms.

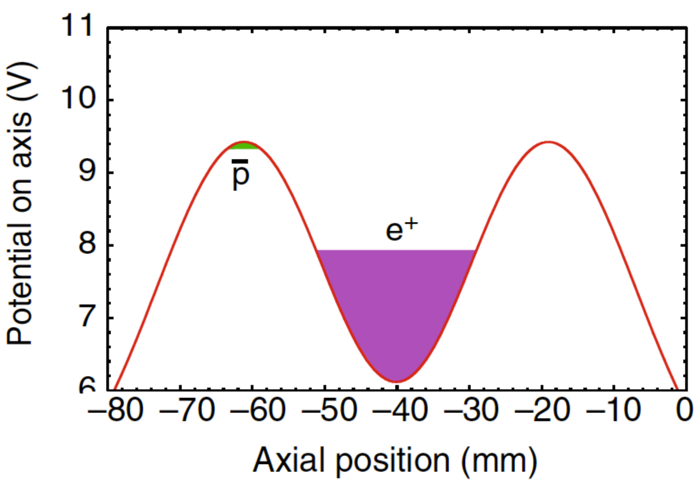

Antihydrogen synthesis

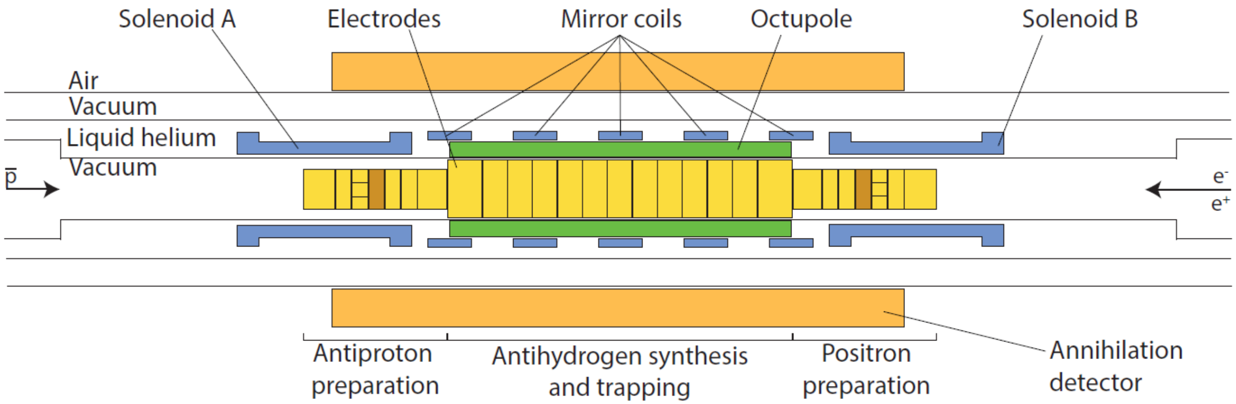

Trap positrons and antiprotons in adjacent potential wells of a Penning-Malmberg trap.

- Slowly merge the particles (in 1s) by lowering the barrier between them.
- We typically mix 3 million positrons (at ~20K) with 90,000 antiprotons (at ~50K) forming around 50,000 antihydrogen atoms.

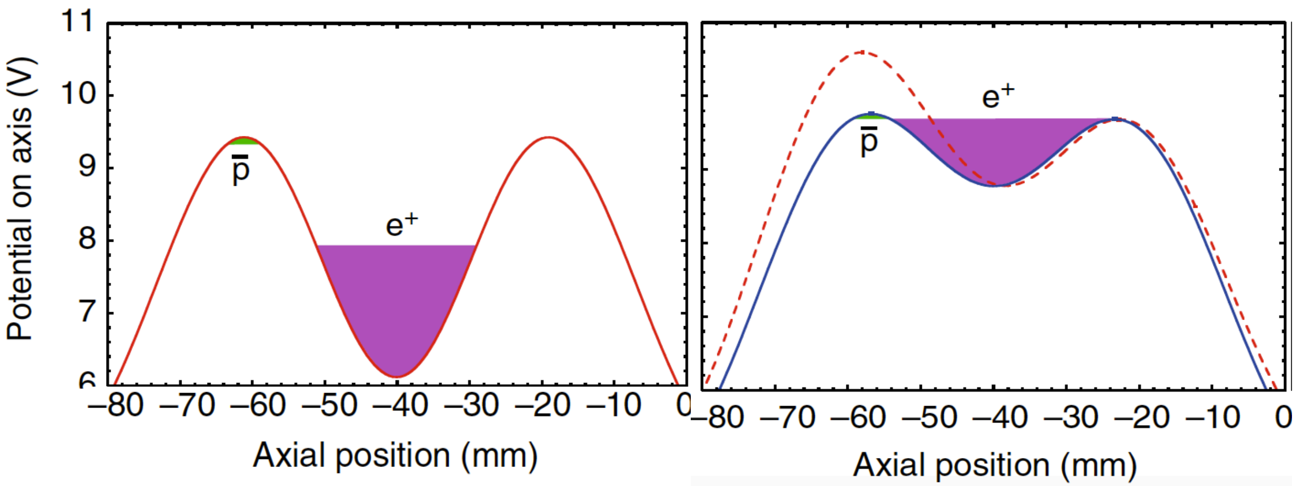

Antihydrogen synthesis

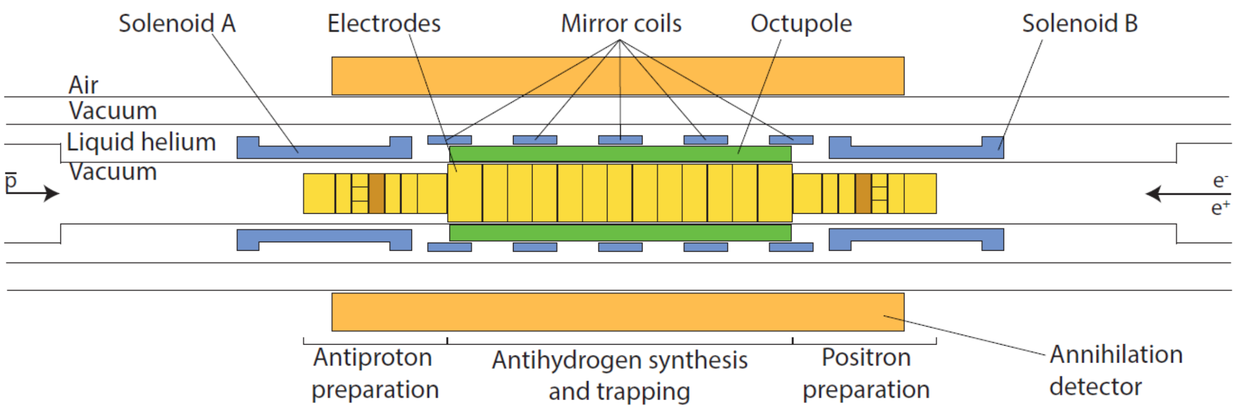

Trap positrons and antiprotons in adjacent potential wells of a Penning-Malmberg trap.

- Slowly merge the particles (in 1s) by lowering the barrier between them.
- We typically mix 3 million positrons (at ~20K) with 90,000 antiprotons (at ~50K) forming around 50,000 antihydrogen atoms.

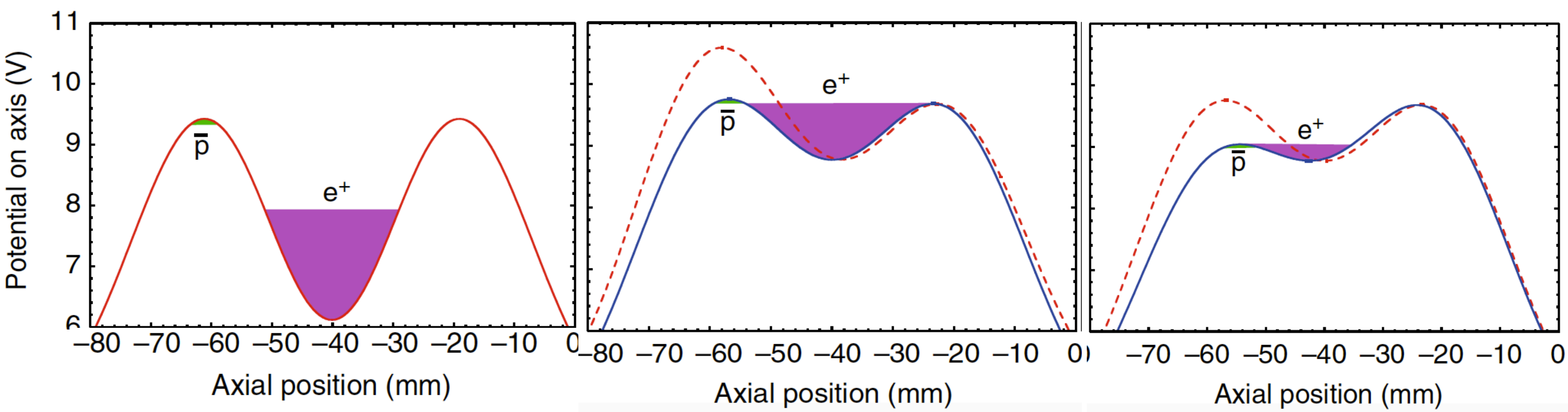

Antihydrogen trapping

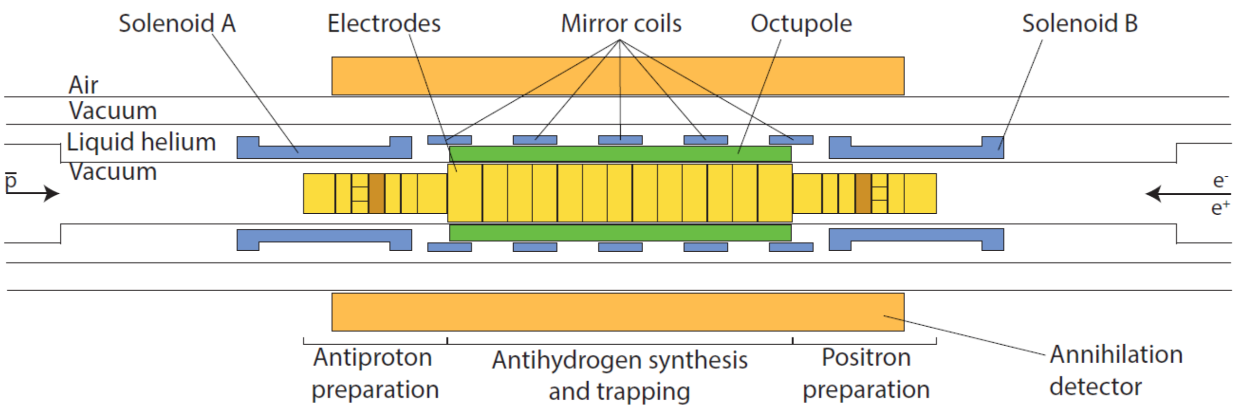

Before mixing the particles, a magnetic minimum trap is energised consisting of an octupole and five mirror coils.

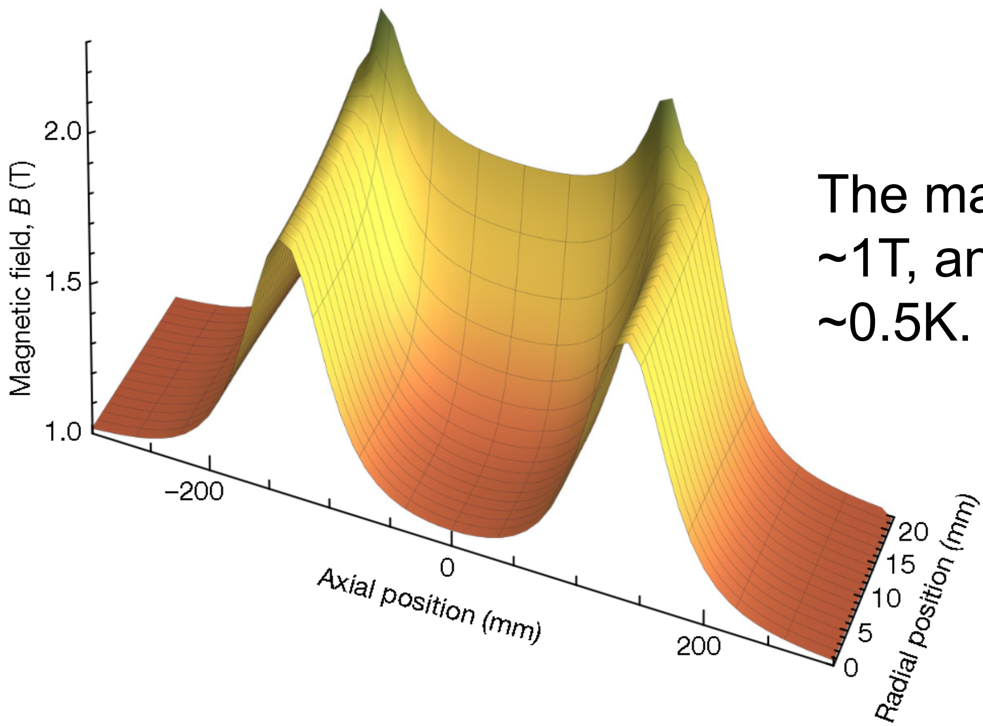

The magnetic field at the trap center is ~1T, and the trap depth corresponds to ~0.5K.

Antihydrogen detection

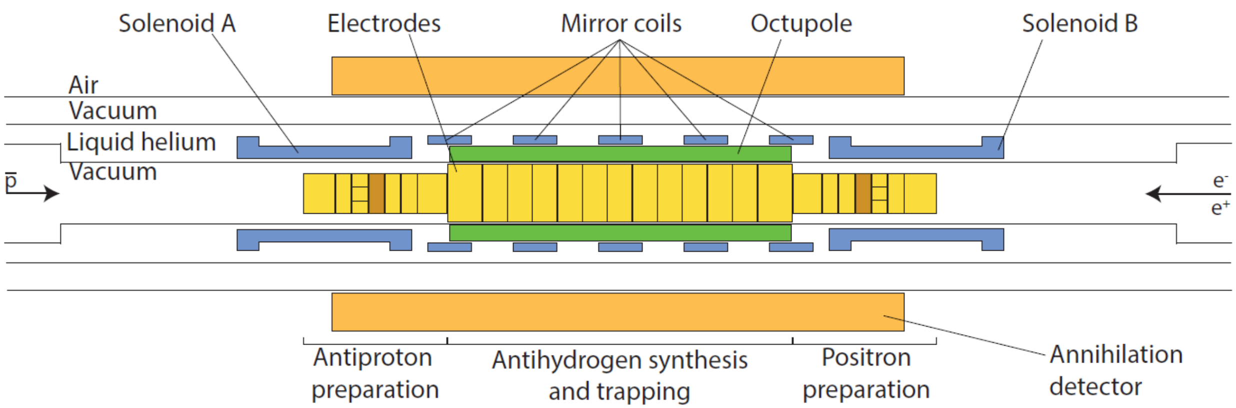

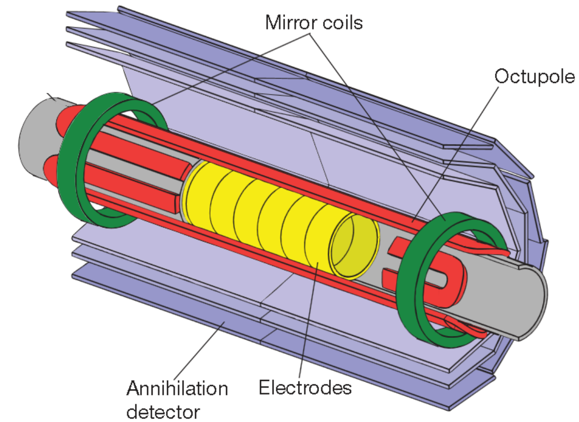

- We detect antihydrogen by ramping down the trap magnets to release the atoms.
- Image the annihilation products with a silicon vertex detector.
- Event topology allows us to distinguish antiproton annihilations from cosmic rays.
- Reconstruction efficiency: 0.69
- Background: 40mHz.

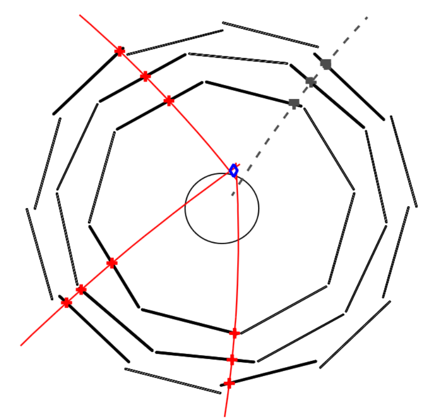

Antihydrogen accumulation

We can accumulate trapped antihydrogen through multiple mixing cycles, and have demonstrated trapping of >1000 atoms in this way.

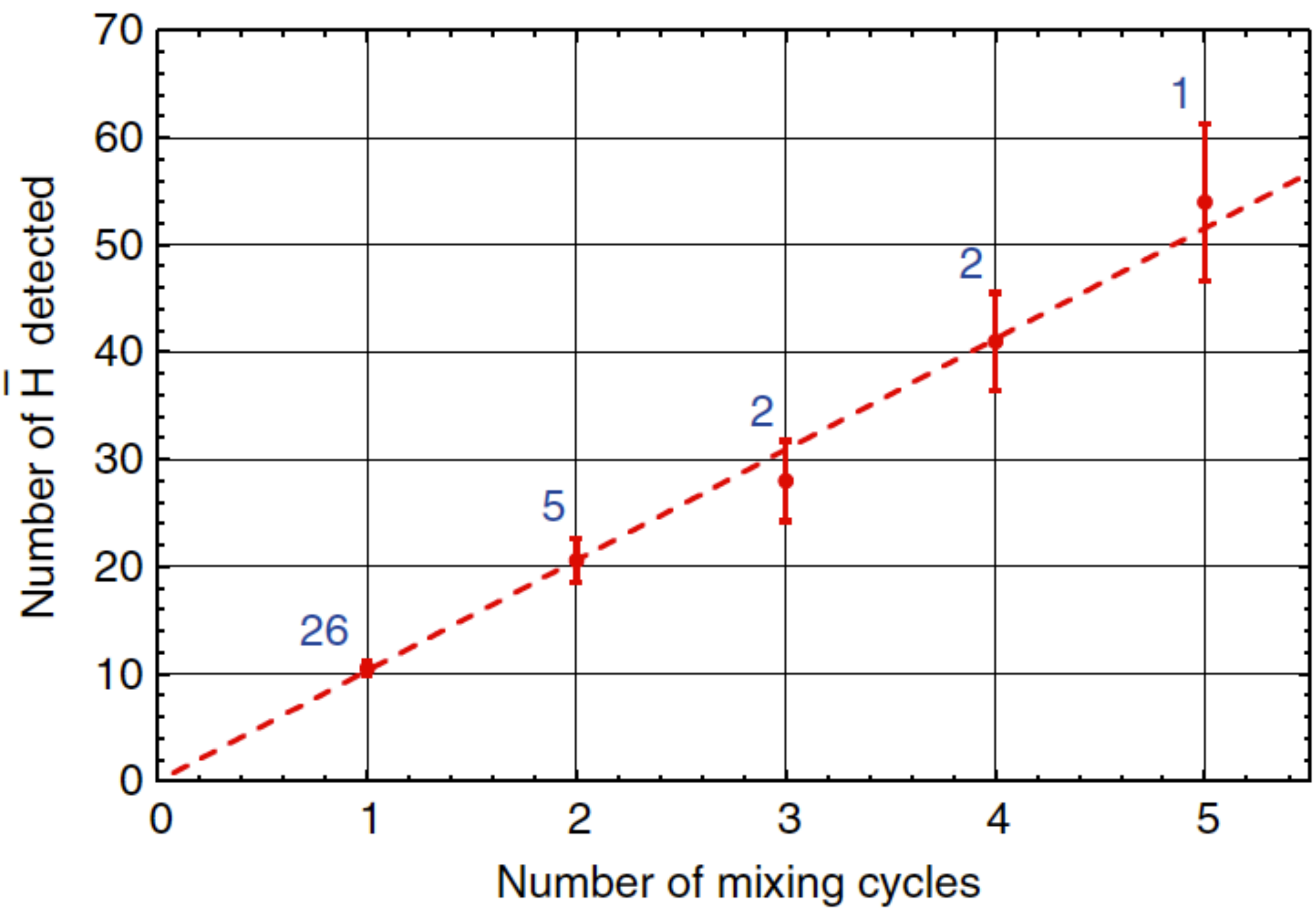

ALPHA Collaboration, Nat. Comms. **8**, 681 (2017).

1S-2S experiment

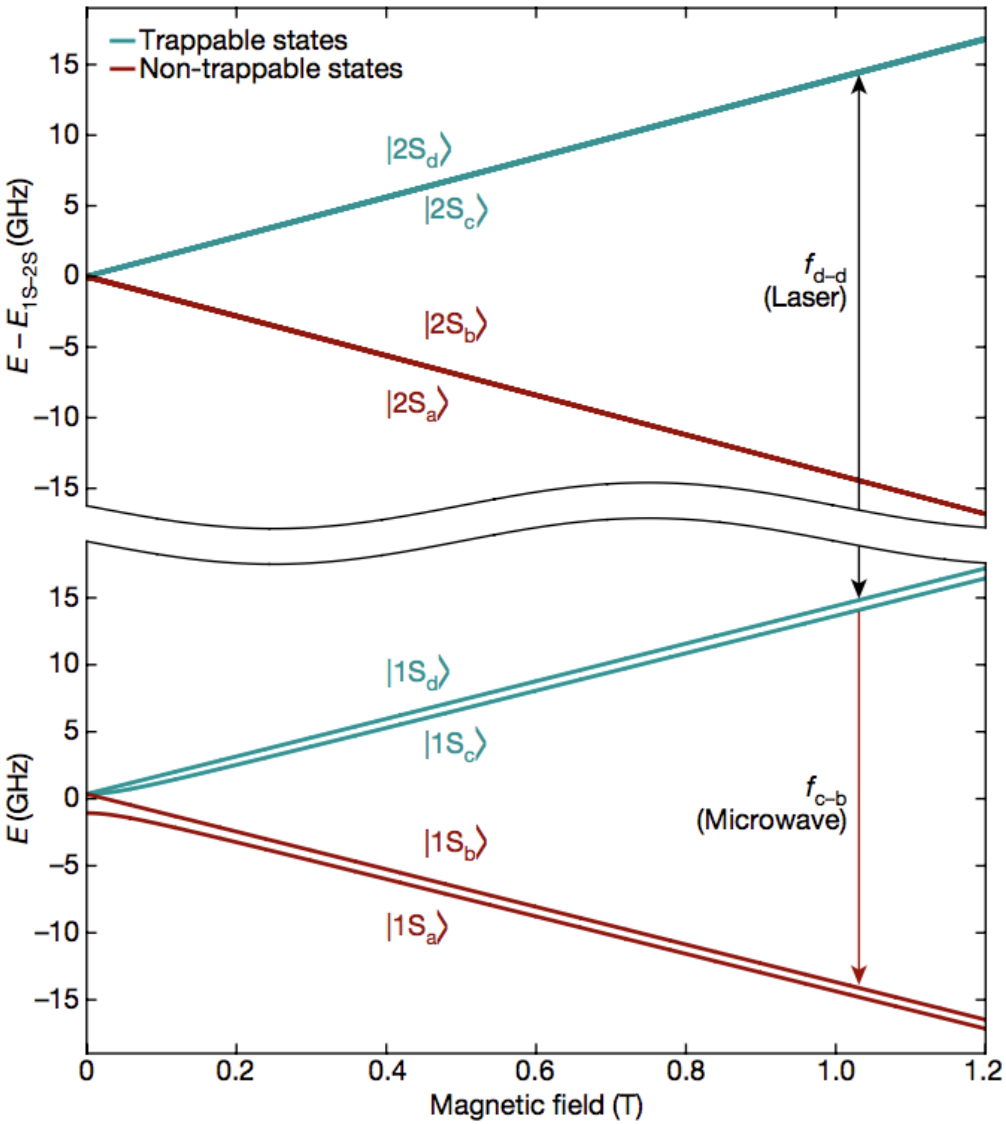

Measure the resonant frequency of the $1S_d$-$2S_d$ transition, and compare with the expected value in hydrogen (in the same trap environment).

We require:
- Knowledge of the magnetic field at the trap center.
- Sufficient laser intensity to excite the two-photon transition (at ~243nm).

1S-2S experiment setup

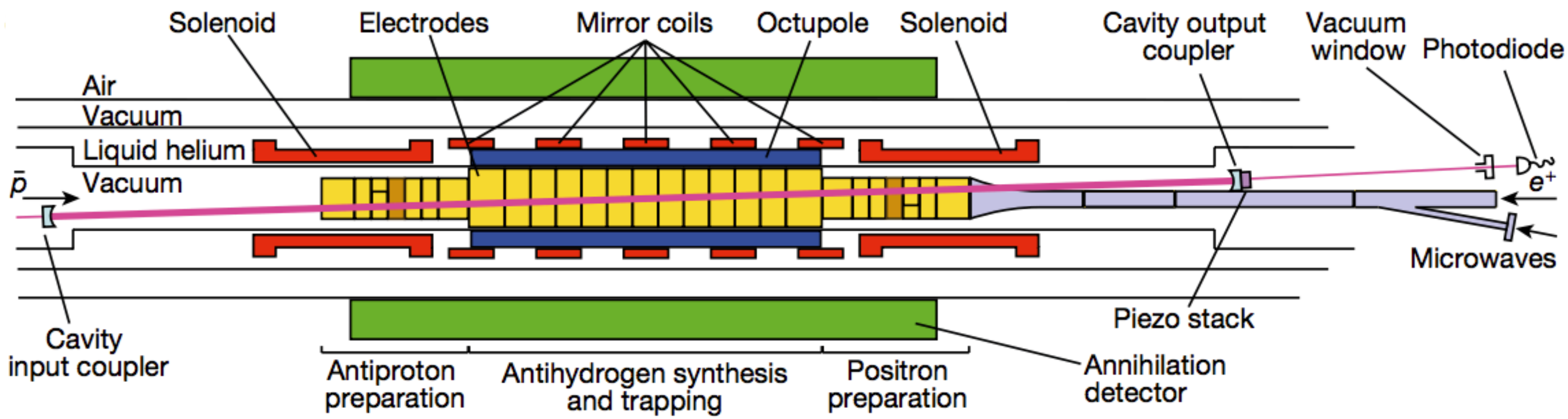

- The 243nm laser is frequency stabilized to a ULE cavity and referenced to a frequency comb.
- The enhancement cavity is locked to the 243nm laser giving 1W of power inside the atom trap.

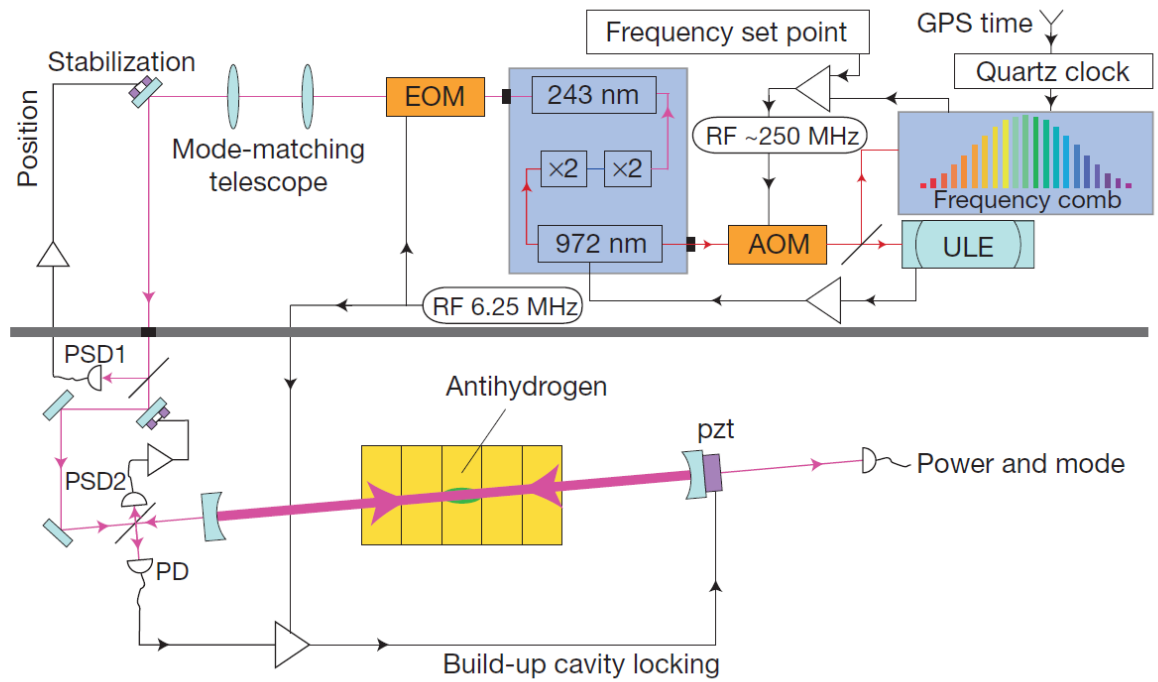

1S-2S experiment procedure

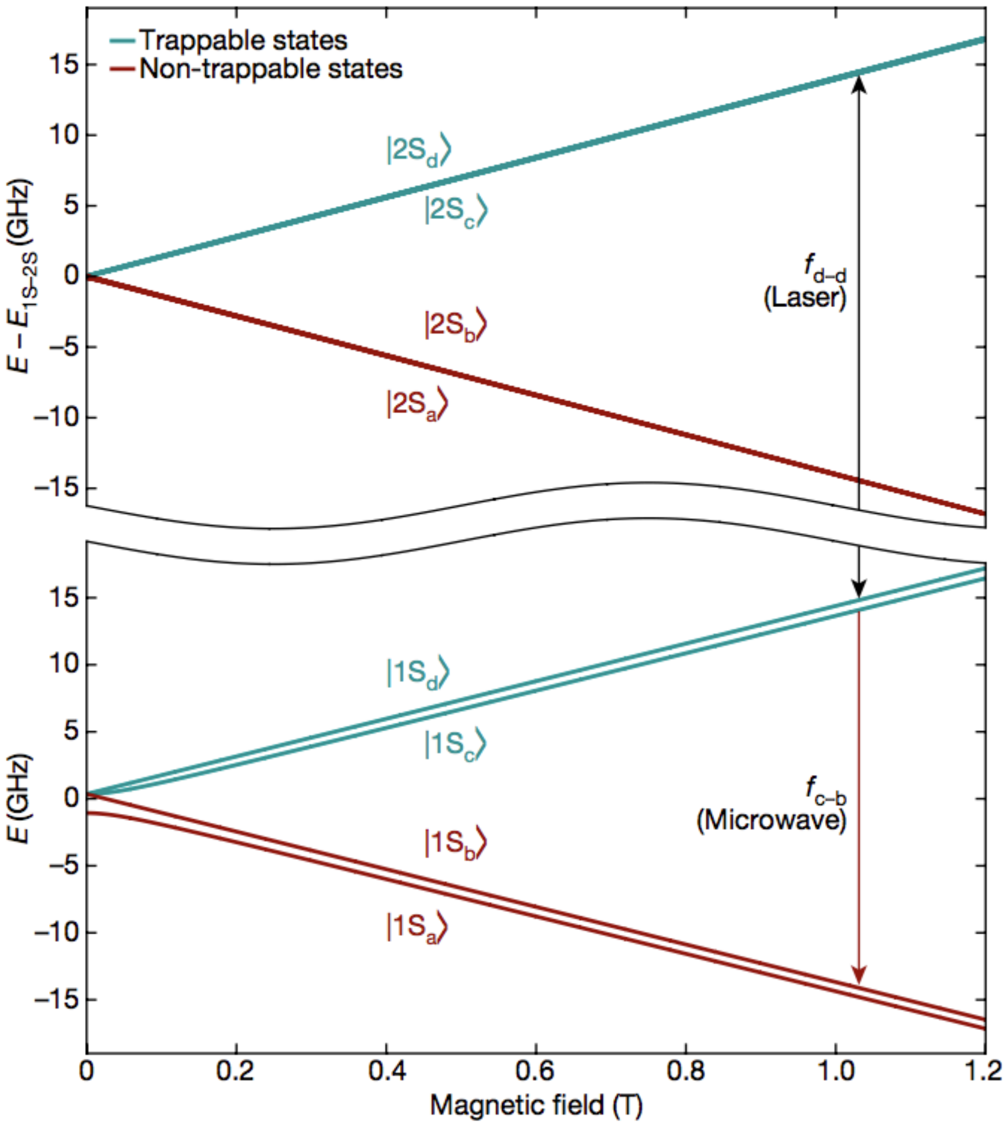

Measure the resonant frequency of the $1S_d$-$2S_d$ transition, by:

- Exposing atoms to light for 300s, at a fixed frequency.
- Look for atoms leaving the trap during laser excitation period (appearance measurement).
- Remove atoms in the $1S_c$ state by driving positron spin-flip transition to the $1S_b$ (non-trappable) state.
- Turn off the trapping field, and measure how many atoms are still in the trap (disappearance measurement).

1S-2S lineshape

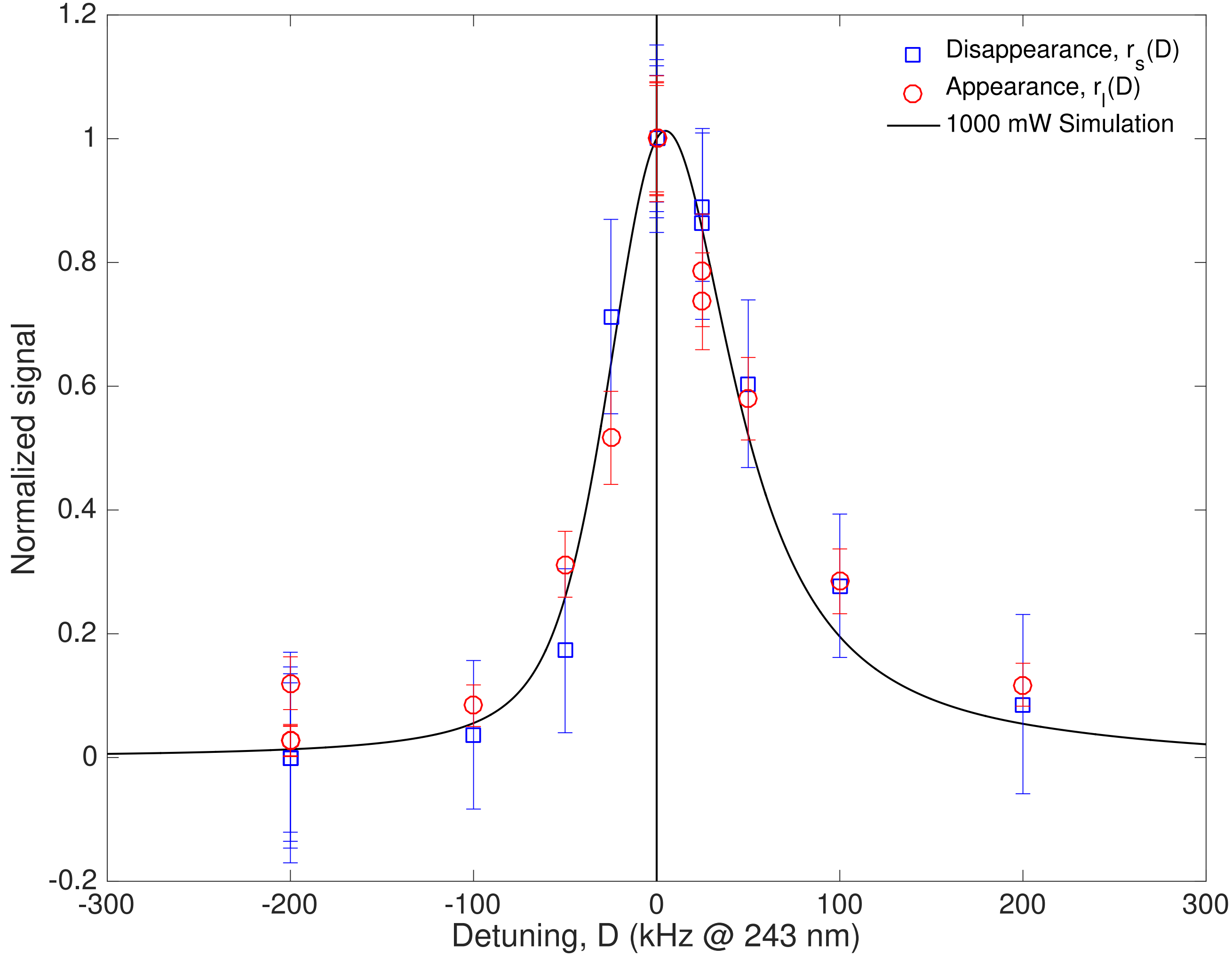

ALPHA Collaboration, Nature **557**, 71 (2018).

1S-2S lineshape

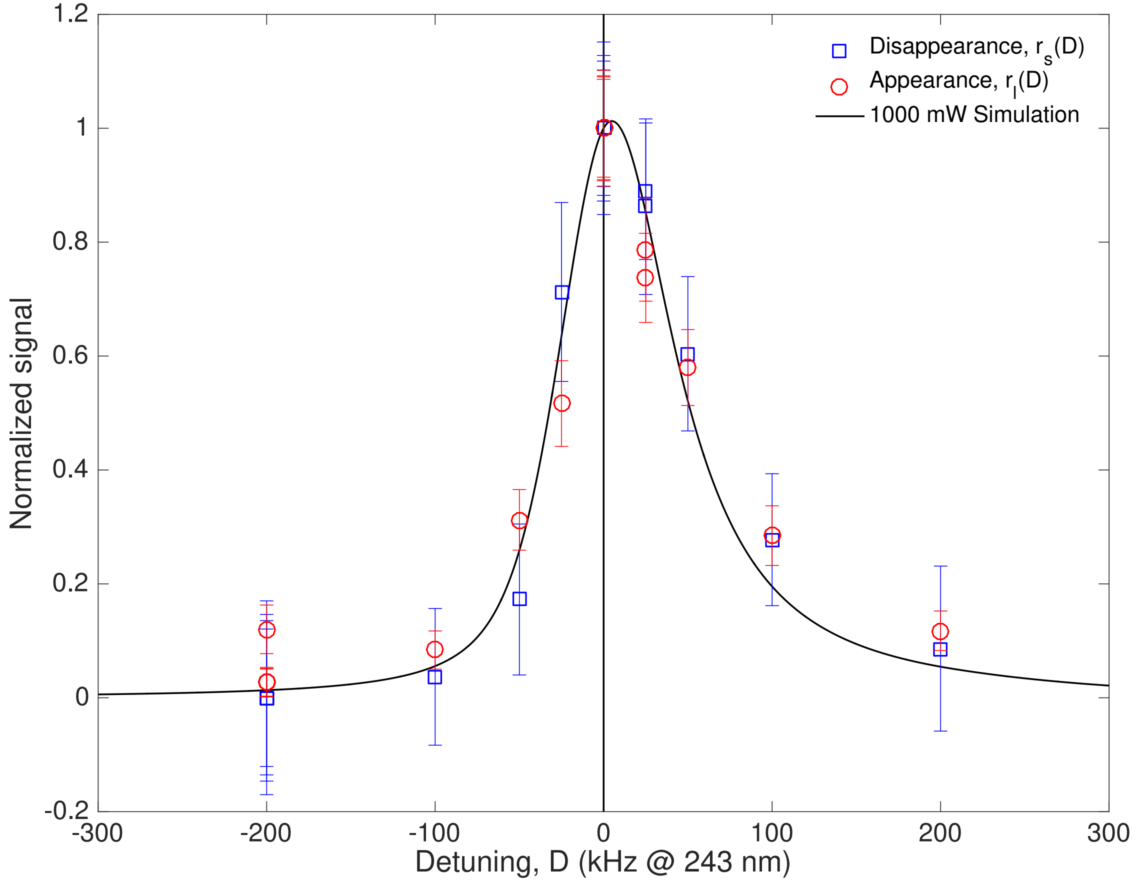

Fit: $f_{\text{d-d}} = 2{,}466{,}061{,}103{,}079.4\ (5.4)$ kHz

Calculated: $f_{\text{d-d}} = 2{,}466{,}061{,}103{,}080.3\ (0.6)$ kHz

ALPHA Collaboration, Nature **557**, 71 (2018).

1S-2S lineshape

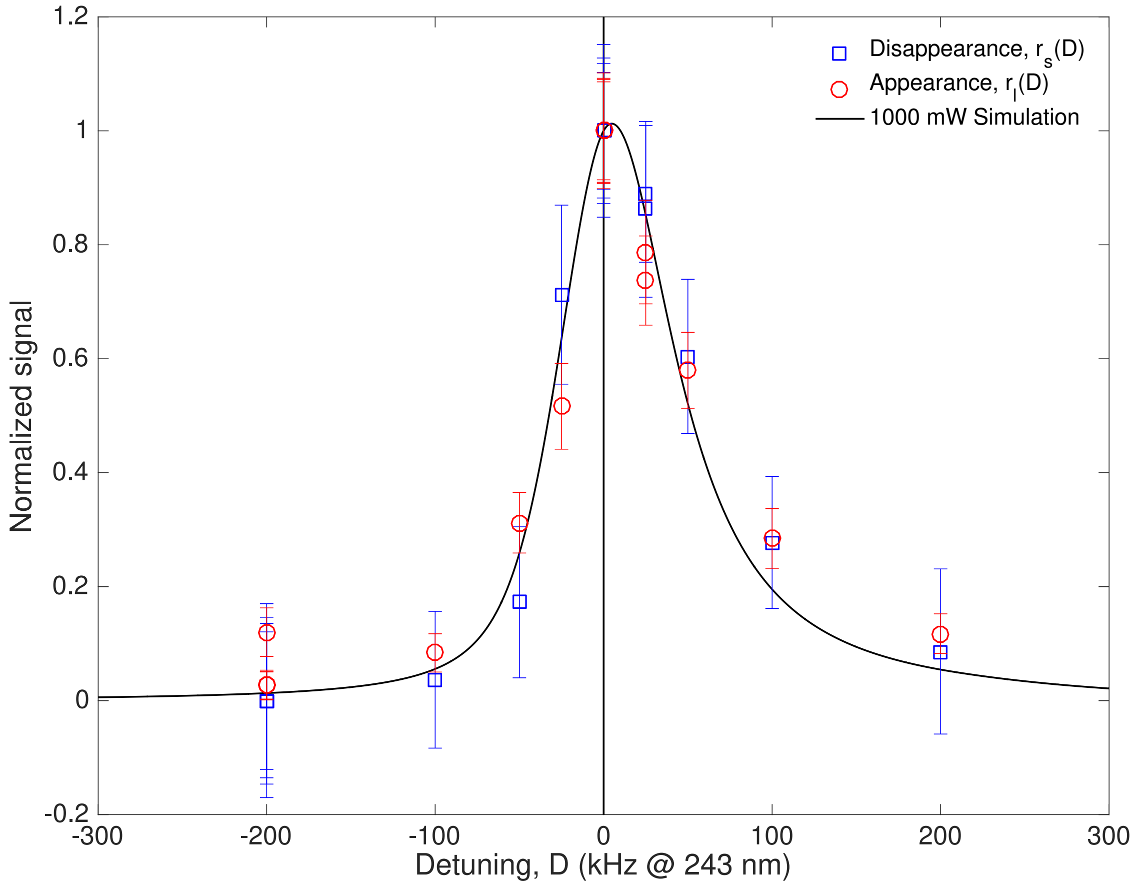

Measured resonance frequency is consistent with the expected resonance frequency in hydrogen, and therefore consistent with CPT invariance, to a precision of 2×10^{-12}.

Measurement of hyperfine splitting

- We inject microwaves at around 28GHz to drive positron spin-flip transitions |c> to |b>, and |d> to |a>.
- Frequency difference between the transitions is the ground-state hyperfine splitting, independent of B-field.

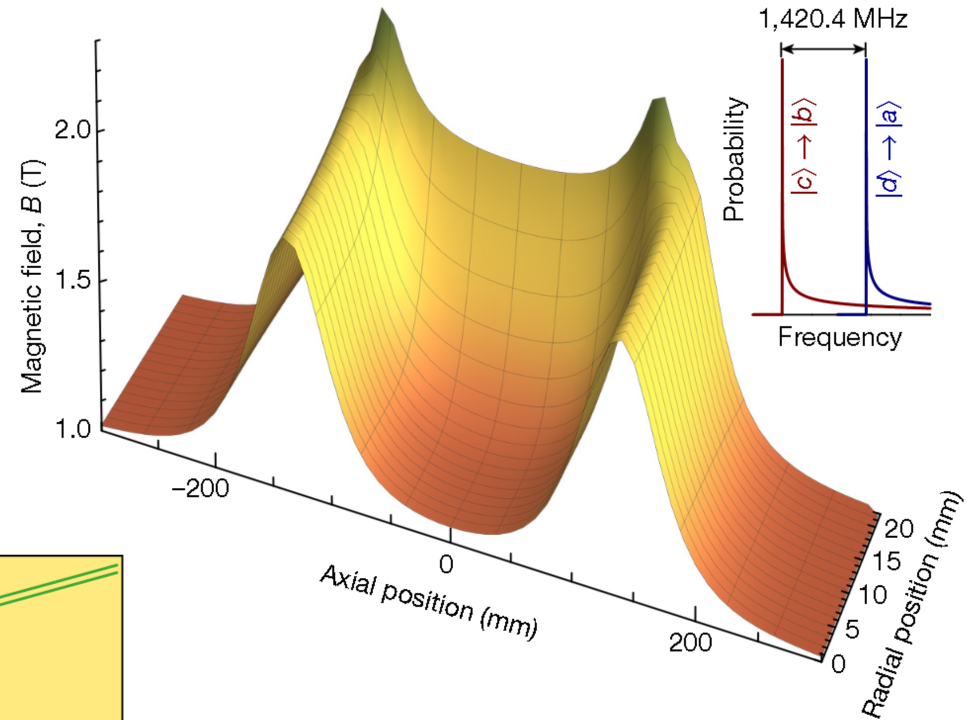

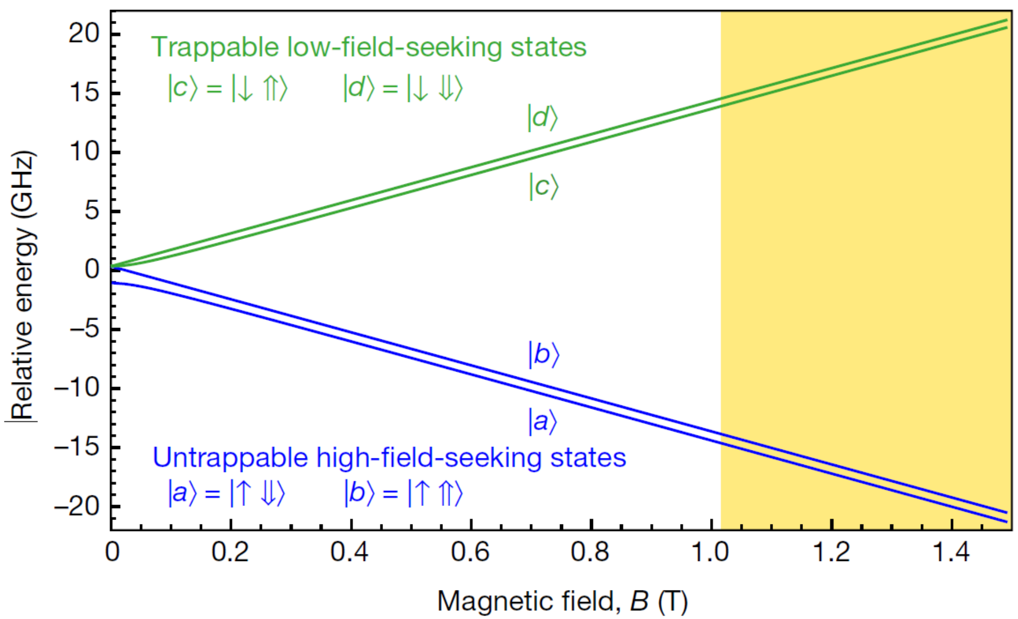

- Due to the highly inhomogeneous magnetic field, the transition lineshapes are strongly broadened.

Ground-State Hyperfine Splitting

- Scan microwave frequency over each transition in 300kHz increments (4s pulses).

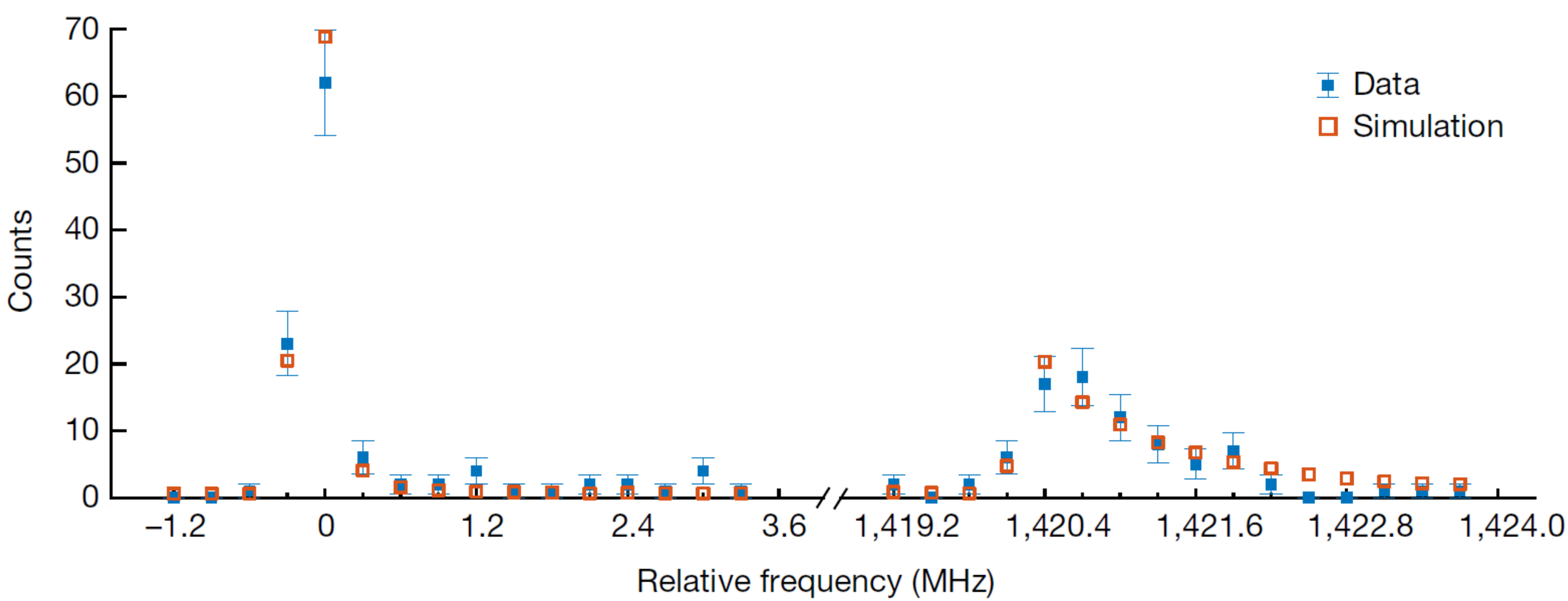

- Determine the ground-state hyperfine splitting from the separation of the onsets of the two transitions to be: **1420.4 ± 0.5 MHz**.

ALPHA Collaboration, Nature **548**, 66-69 (2017).

Outlook

- Laser cooling of antihydrogen.
- Improved precision measurement of the 1S-2S resonance frequency.
- Gravitational measurements on antihydrogen: the ALPHA collaboration is currently constructing a new experiment (ALPHA-g) where we will study the free-fall of antihydrogen in a vertical trap.

Matter-antimatter comparisons

ALPHA

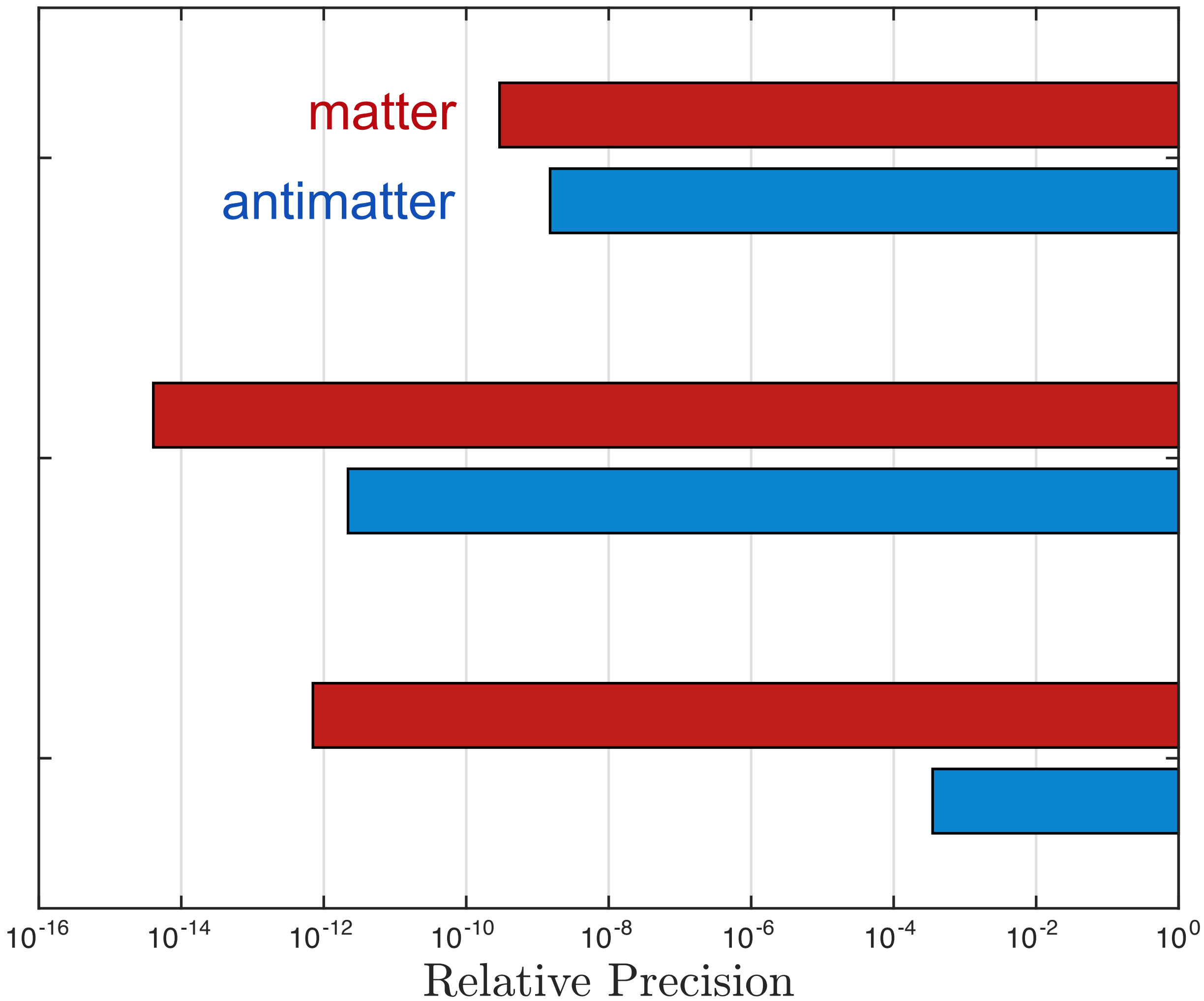

G. Schneider *et al.*, Science **358**, 1081 (2017)

(anti)proton g-factor

C. Smorra *et al.*, Nature **550**, 371 (2017)

A. Matveev et al., Phys. Rev. Lett. **110**, 230801 (2013)

(anti)hydrogen 1S-2S

M. Ahmadi *et al.*, Nature **557**, 71 (2018)

N. F. Ramsey, Rev. Mod. Phys. **62**, 541 (1990)

(anti)hydrogen GS HFS

M. Ahmadi *et al.*, Nature **548**, 66 (2017)

Thank you for your attention!

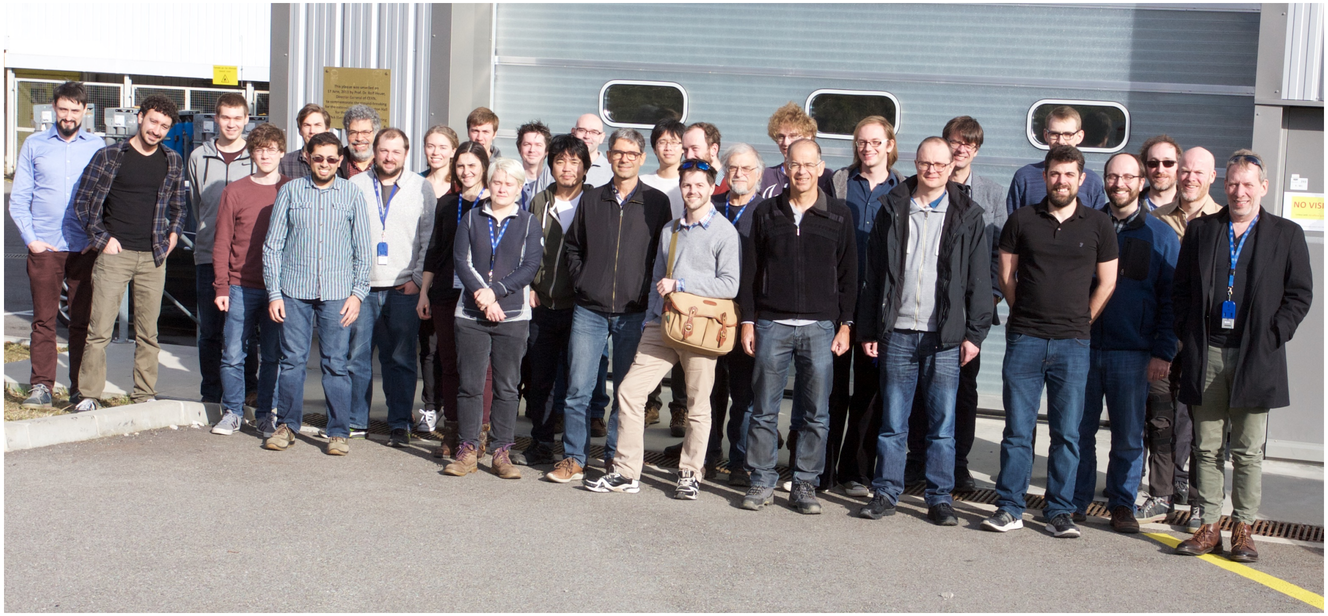

AARHUS UNIVERSITET

UNIVERSITY OF LIVERPOOL

THE UNIVERSITY OF CALIFORNIA BERKELEY · LET THERE BE LIGHT · 1868

BERKELEY LAB

SFU
SIMON FRASER UNIVERSITY
THINKING OF THE WORLD

UNIVERSITY OF CALGARY

Stockholm University

The Cockcroft Institute of Accelerator Science and Technology

MANCHESTER 1824

TRIUMF

NRCN
Nuclear Research Center Negev

SOREQ

PURDUE UNIVERSITY

UNIVERSIDADE DO BRASIL

Swansea University
Prifysgol Abertawe

UBC
THE UNIVERSITY OF BRITISH COLUMBIA

YORK UNIVERSITÉ UNIVERSITY

Additional slides: 1S-2S

	Laser detuning, *D* (kHz)	Number of trials	Atoms lost during laser exposure, *L*	Atoms lost during microwave exposure, *M*	Surviving atoms, *S*	Initially trapped atoms, N_I
Set 1	−200	21	7±7	383±23	504±25	894±35
	−100	21	22±9	415±24	494±24	931±35
	0	21	264±24	423±24	217±16	904±38
	+100	21	75±14	411±23	424±23	910±35
Set 2	−200	21	26±9	394±23	466±24	886±34
	−25	21	113±16	423±24	326±20	862±35
	0	21	219±22	390±23	269±18	878±37
	+25	21	173±20	438±24	296±19	907±37
Set 3	−200	23	8±7	354±22	479±24	841±33
	0	23	303±26	454±25	248±17	1,005±40
	+50	23	176±20	390±23	339±20	905±37
	+200	23	36±11	446±24	459±23	941±35
Set 4	−200	21	7±7	525±26	541±25	1,073±37
	−50	21	86±15	475±25	495±24	1,056±38
	0	21	274±25	480±25	275±18	1,029±40
	+25	21	202±21	516±26	305±19	1,023±38
Total		344	1,991	6,917	6,137	15,045

$$r_l(D) = L(D)/L(0) \qquad r_s(D) = [S(-200\text{kHz}) - S(D)]/[S(-200\text{kHz}) - S(0)]$$

Additional slides: Error budget 1S-2S

Type of uncertainty	Estimated size (kHz)	Comment
Statistical uncertainties	3.8	Poisson errors and curve fitting to measured data
Modelling uncertainties	3	Fitting of simulated data to piecewise-analytic function
Modelling uncertainties	1	Waist size of the laser, antihydrogen dynamics
Magnetic-field stability	0.03	From microwave removal of $1S_c$-state atoms (see text)
Absolute magnetic-field measurement	0.6	From electron cyclotron resonance
Laser-frequency stability	2	Limited by GPS clock
d.c. Stark shift	0.15	Not included in simulation
Second-order Doppler shift	0.08	Not included in simulation
Discrete frequency choice of measured points	0.36	Determined from fitting sets of pseudo-data
Total	5.4	

The estimated statistical and systematic errors (at 121 nm) are tabulated.

Additional slides: power dependence 1S-2S

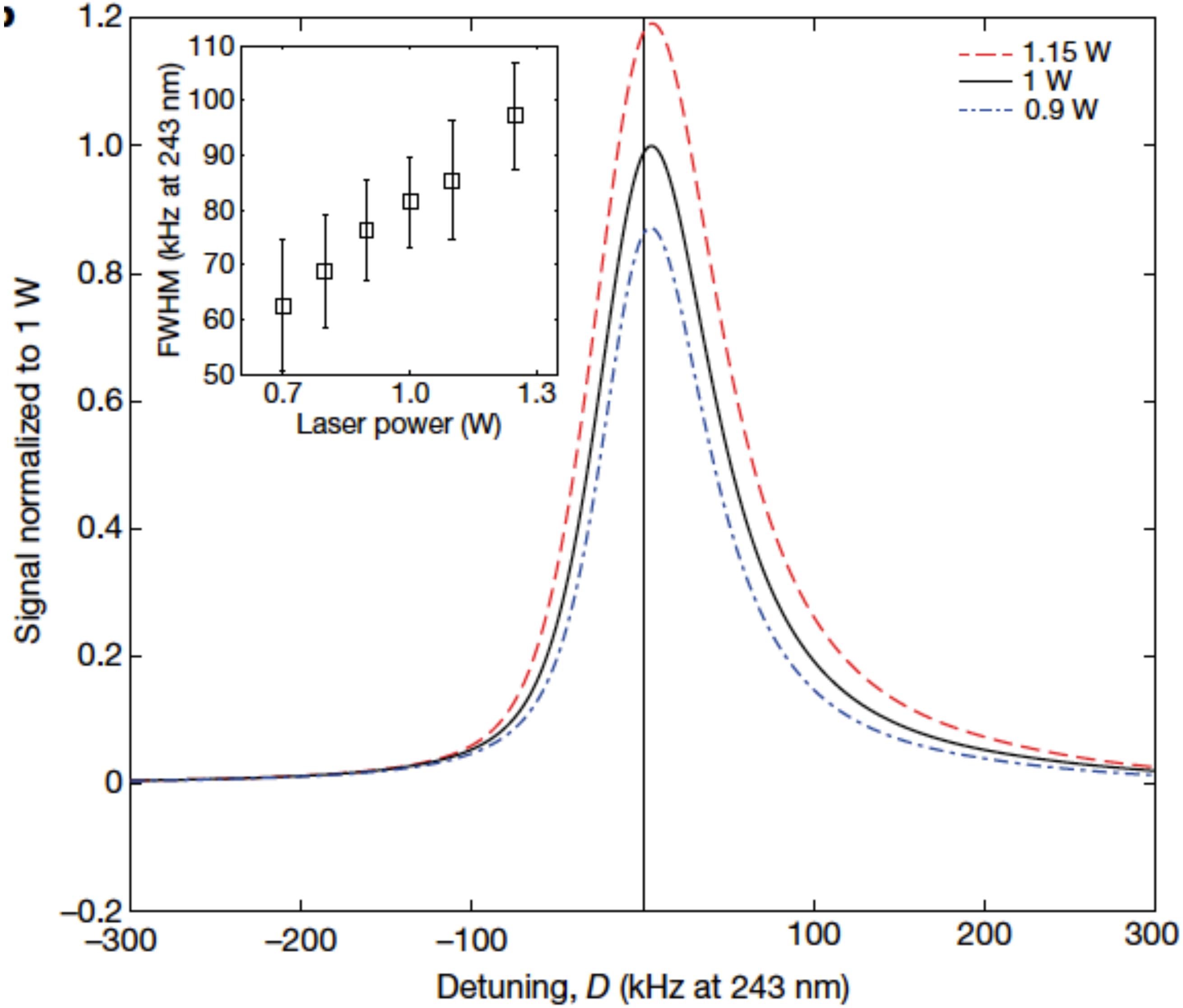

Additional slides: Relative precision

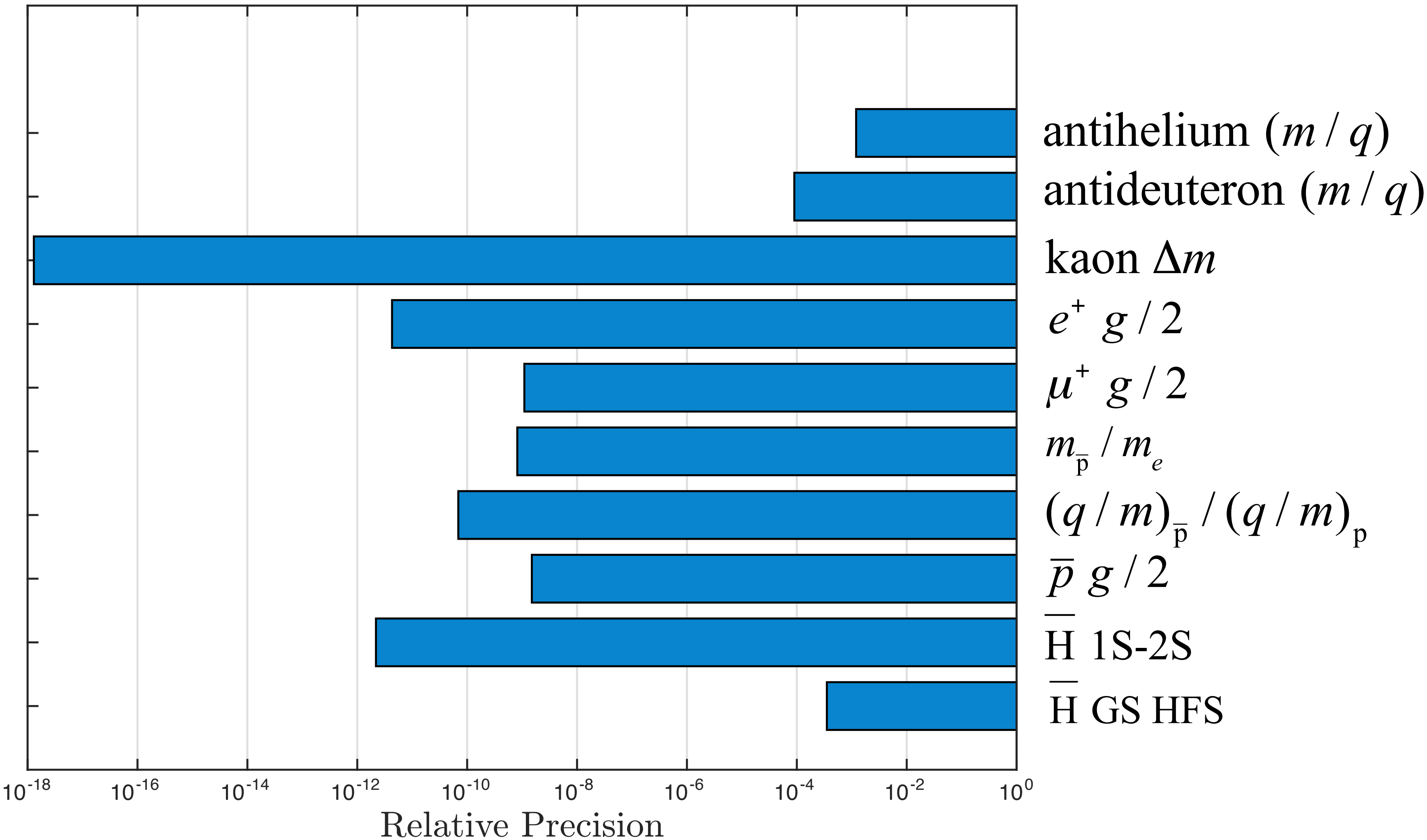

Additional slides: Energy Sensitivity

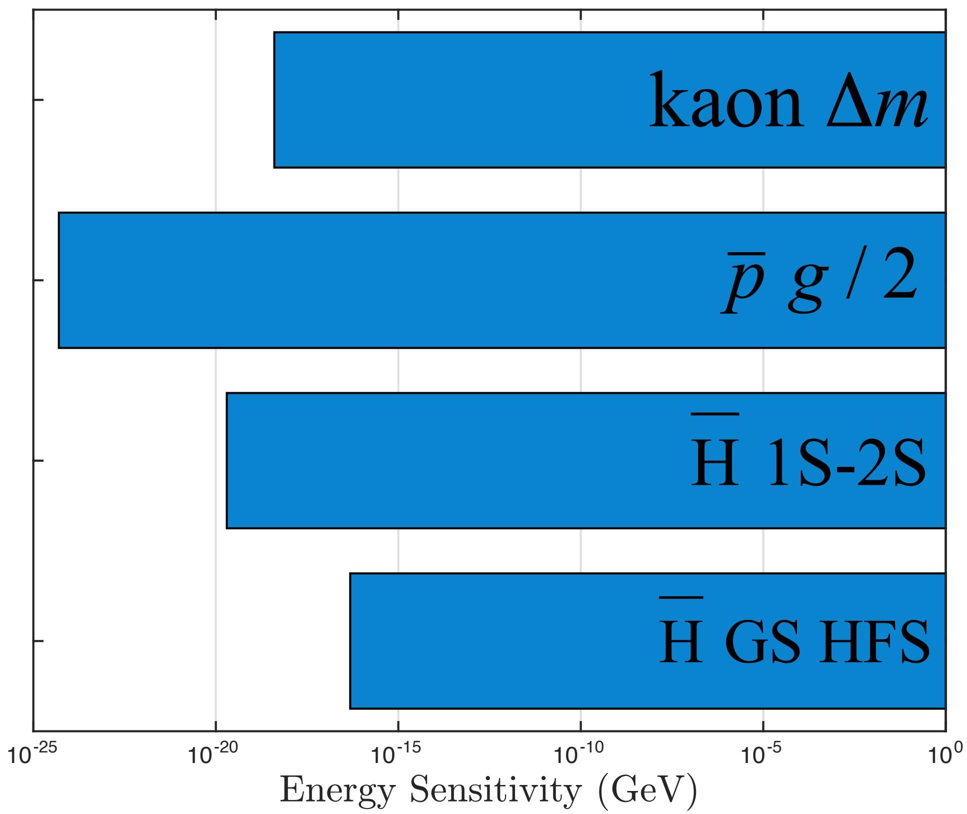

B. Schwingenheuer *et. al.*, Phys. Rev. Lett **74** 4376 (1995)

C. Smorra *et al.*, Nature **550**, 371 (2017)

M. Ahmadi *et al.*, Nature **557**, 71 (2018)

M. Ahmadi *et al.*, Nature **548**, 66 (2017)